

UC Irvine

UC Irvine Previously Published Works

Title

Active repression by RAR γ signaling is required for vertebrate axial elongation

Permalink

<https://escholarship.org/uc/item/2jj8b9rz>

Journal

Development, 141(11)

ISSN

0950-1991

Authors

Janesick, Amanda
Nguyen, Tuyen TL
Aisaki, Ken-ichi
[et al.](#)

Publication Date

2014-06-01

DOI

10.1242/dev.103705

Copyright Information

This work is made available under the terms of a Creative Commons Attribution-NonCommercial-NoDerivatives License, available at <https://creativecommons.org/licenses/by-nc-nd/4.0/>

Peer reviewed

RESEARCH ARTICLE

Active repression by RAR γ signaling is required for vertebrate axial elongation

Amanda Janesick¹, Tuyen T. L. Nguyen¹, Ken-ichi Aisaki², Katsuhide Igarashi², Satoshi Kitajima², Roshantha A. S. Chandraratna³, Jun Kanno² and Bruce Blumberg^{1,4,*}

ABSTRACT

Retinoic acid receptor gamma 2 (RAR γ 2) is the major RAR isoform expressed throughout the caudal axial progenitor domain in vertebrates. During a microarray screen to identify RAR targets, we identified a subset of genes that pattern caudal structures or promote axial elongation and are upregulated by increased RAR-mediated repression. Previous studies have suggested that RAR is present in the caudal domain, but is quiescent until its activation in late stage embryos terminates axial elongation. By contrast, we show here that RAR γ 2 is engaged in all stages of axial elongation, not solely as a terminator of axial growth. In the absence of RA, RAR γ 2 represses transcriptional activity *in vivo* and maintains the pool of caudal progenitor cells and presomitic mesoderm. In the presence of RA, RAR γ 2 serves as an activator, facilitating somite differentiation. Treatment with an RAR γ -selective inverse agonist (NRX205099) or overexpression of dominant-negative RAR γ increases the expression of posterior Hox genes and that of marker genes for presomitic mesoderm and the chordoneural hinge. Conversely, when RAR-mediated repression is reduced by overexpressing a dominant-negative co-repressor (c-SMRT), a constitutively active RAR (VP16-RAR γ 2), or by treatment with an RAR γ -selective agonist (NRX204647), expression of caudal genes is diminished and extension of the body axis is prematurely terminated. Hence, gene repression mediated by the unliganded RAR γ 2-co-repressor complex constitutes a novel mechanism to regulate and facilitate the correct expression levels and spatial restriction of key genes that maintain the caudal progenitor pool during axial elongation in *Xenopus* embryos.

KEY WORDS: Active repression, Axial elongation, Chordoneural hinge, Posterior Hox, Presomitic mesoderm, Retinoic acid receptor

INTRODUCTION

Repression mediated through unliganded retinoic acid receptors (RARs) is an important yet understudied function exhibited by nuclear receptors (reviewed by Weston et al., 2003). Although RA plays a major role in patterning the hindbrain, retina, placodes and somites, its absence is crucial for the development of structures found at the head and tail of the embryo. RARs exhibit basal repression in the absence of ligand, binding constitutively to their targets, recruiting co-repressors, and actively repressing the basal

transcriptional machinery (Chen and Evans, 1995). When ligand is present, co-repressors are replaced by co-activators and target genes are transcribed (Chakravarti et al., 1996).

We previously demonstrated that repression mediated through unliganded RARs was important for anterior neural patterning, establishing a novel role for RAR as a repressor *in vivo* (Koide et al., 2001). Overexpression of a dominant-negative RAR α expanded anterior and midbrain markers caudally and shifted somitomeres rostrally (Blumberg et al., 1997; Moreno and Kintner, 2004). Exogenous RA, constitutively active RAR α or derepression of RAR α produced the opposite effect: severe anterior truncations, diminished anterior markers, and anteriorly shifted midbrain and hindbrain markers. Stabilization of co-repressors resulted in enhanced anterior neural structures and posteriorly shifted mid/hindbrain markers (Koide et al., 2001).

Axial elongation requires continual replenishing of bipotential caudal progenitor cells (maintained by Wnt and FGF signaling, but inhibited by RA) that give rise to notochord, neural tube and somites (Cambray and Wilson, 2002; Davis and Kirschner, 2000). The most stem-like cells are located in the chordoneural hinge (CNH), where the posterior neural plate overlies the caudal notochord (Beck and Slack, 1998). Cells from the CNH contribute to presomitic mesoderm (PSM), which supplies committed somitic precursor cells to the rostral determination wavefront (reviewed by Dequeant and Pourquie, 2008). PSM is initially homogenous and unorganized [expressing *Mesogenin1* (*Msgn1*) and *Tbx6*], then becomes patterned into somitomeres marked by *Thylacine2* (*Thyl2*) and *Ripply2* (reviewed by Dahmann et al., 2011). Epithelialization of presomitic domains results in mature somites (Nakaya et al., 2004).

RA is well known to function in the trunk, where it promotes differentiation of PSM into somitomeres (Moreno and Kintner, 2004). By contrast, RA is actively metabolized and cleared by CYP26A1 in the caudal region (Fujii et al., 1997). Treatment with RA leads to loss of posterior structures (Sive et al., 1990); *Cyp26a1*^{-/-} mice exhibit posterior truncations and homeotic vertebral transformations (Abu-Abed et al., 2001; Sakai et al., 2001). Exposing embryos to RA inhibits proliferation of axial progenitor cells in CNH and PSM, leading to axial truncation from premature exhaustion of the progenitor pool (Gomez and Pourquie, 2009). Therefore, RA is normally excluded from unsegmented mesenchyme in PSM and the CNH. RAR γ is expressed at high levels throughout the entire caudal region, including CNH and PSM (Mollard et al., 2000; Pfeffer and De Robertis, 1994), yet, based on *Cyp26a1* expression, RA is absent (de Roos et al., 1999). The physiological significance of RAR γ expression in the embryonic posterior is uncertain. RAR γ might function to terminate the body axis at late stages by inducing apoptosis (Olivera-Martinez et al., 2012), but that model would not explain the strong expression of RAR γ observed at neurula, continuing through tailbud stages, despite the apparent absence of RA.

¹Department of Developmental and Cell Biology, 2011 Biological Sciences 3, University of California, Irvine, CA 92697-2300, USA. ²Division of Cellular and Molecular Toxicology, Biological Safety Research Center, National Institute of Health Sciences, 1-18-1 Kamiyoga, Setagaya-ku, Tokyo 158-8501, Japan. ³IO Therapeutics, Santa Ana, CA 92705-5851, USA. ⁴Department of Pharmaceutical Sciences, University of California, Irvine, CA 92697-2300, USA.

*Author for correspondence (blumberg@uci.edu)

Rary2 skirts the posterior edge of the determination wavefront and is co-expressed with PSM, CNH and posterior Hox markers. We hypothesized that *Rary2* serves a dual function: as an activator in somite differentiation but a repressor in the maintenance of PSM and the caudal progenitor pool. Loss of RAR γ 2 severely shortens the embryo body axis and inhibits somitogenesis. Loss of RAR γ 2 expands the anterior border of PSM expression near the wavefront (where activation is lost), but diminishes the expression domain of caudal PSM and posterior Hox genes (where repression is lost). Increasing RAR-mediated repression expands the expression of posterior Hox, PSM and CNH markers, creating smaller somite domains via an indirect, 'repressing a repressor' mechanism. Relief of repression results in a truncated body axis with decreased PSM and CNH markers. Axial extension and segmentation in vertebrates relies on the maintenance of unsegmented PSM mesenchyme and replenishing of caudal progenitor cells. Our data show that RAR γ 2 plays a crucial role in this process, repressing target genes to maintain PSM and caudal progenitors in the absence of RA, while activating others to promote somitogenesis in the presence of RA.

RESULTS

Posterior Hox, PSM and CNH genes are upregulated by RAR inverse agonist

We showed previously that active repression of RAR target genes by unliganded RAR is required for head formation (Koide et al., 2001). Treatment with the pan-RAR inverse agonist AGN193109 increased the expression of genes involved in patterning anterior neural structures, whereas treatment with pan-RAR agonist TTNPB decreased the expression of anterior marker and cement gland-specific genes (Koide et al., 2001), revealing a set of genes specifically upregulated/downregulated by TTNPB (Arima et al., 2005). Validation studies identified a subset upregulated by AGN193109. We hypothesized that active repression by unliganded RARs is biologically important and designed an experiment to identify genes upregulated or downregulated by modulating repression. Percellome analysis (Kanno et al., 2006) quantified the copy number per embryo of all genes represented on Affymetrix *Xenopus* microarray v1.0. Among these we identified a collection of genes linked to the maintenance of caudal axial progenitors that were downregulated by TTNPB and upregulated by AGN193109 (Table 1). RAR-mediated repression upregulates the steady-state expression of posterior Hox paralogs 9-13 and genes found in both unsegmented PSM and CNH.

Thus, we hypothesized that RAR is a repressor required for axial elongation.

Xenopus RARs repress basal transcription in the absence of ligand

The ability of unliganded RARs to behave as repressors is well documented, although not all human receptor subtypes can recruit co-repressors (e.g. SMRT) in the absence of ligand (Wong and Privalsky, 1998). We tested the ability of *Xenopus* RAR (xRAR) subtypes to repress basal activity of a luciferase-dependent reporter using the GAL4-RAR system (supplementary material Fig. S1D-F) (Blumberg et al., 1996). *Xenopus* RAR α , RAR β and RAR γ suppressed basal activity *in vitro* and *in vivo* (supplementary material Fig. S1A,C), whereas human RAR β and RAR γ did not (supplementary material Fig. S1B). Thus, xRARs can function as repressors in the absence of ligand.

Rary2 is expressed in the PSM and CNH but is mostly absent from the trunk

Whole-mount *in situ* hybridization (WISH) revealed that *Rary2* is the predominant isoform expressed in the *Xenopus* embryonic posterior (supplementary material Fig. S2A). In late neurula and early tailbud stage embryos, *Rary2* is strongly expressed in the anterior and posterior, but almost undetectable in the trunk. *Rary2* expression later becomes pronounced in the tail and head, particularly in hyoid, branchial and mandibular neural crest. *Rary1* is expressed similarly. QPCR analysis revealed that *Rary2* is 1000- to 4000-fold more abundant than *Rary1* at stages 10-22, and 100- to 400-fold more abundant at all other stages analyzed (supplementary material Fig. S2B). Subsequent experiments utilized *Rary2*-selective reagents. We conclude that *Rary2* is the predominant isoform expressed in the posterior region of embryos.

Rary2 is expressed where RA is probably absent (owing to CYP26A1 expression). Key posterior genes were upregulated by AGN193109. We hypothesized that RAR γ 2 posterior to the wavefront is a repressor, maintaining unsegmented PSM and the progenitor cell pool required for axial elongation. We used double WISH to compare the expression of *Rary2* with that of *Hoxc10*, an important member of the Abd-B Hox gene family promoting caudal development over thorax (Lamka et al., 1992). *Rary2* expression completely overlaps caudal *Hoxc10* expression (Fig. 1E,H) but not the anteriormost neural or lateral plate expression of *Hoxc10* (Fig. 1E,H). These data position

Table 1. Percellome analysis reveals that posterior Hox, PSM and CNH markers are upregulated by RAR inverse agonist

Unigene	109 (fold)	<i>P</i>	TTN (fold)	<i>P</i>	Symbol	Gene name	Cat
Xl.72193	3.57	2.11×10 ⁻³	0.19	5.77×10 ⁻⁴	<i>Hoxc13</i>	Homeobox C13	PP
Xl.266	3.47	4.26×10 ⁻³	0.12	2.26×10 ⁻⁴	<i>Hoxa11</i>	Homeobox A11	PP
Xl.21864	3.15	2.03×10 ⁻³	0.22	2.68×10 ⁻⁴	<i>Hoxc10</i>	Homeobox C10	PP
Xl.72292	3.02	7.32×10 ⁻³	0.16	1.62×10 ⁻⁴	<i>Hoxd9</i>	Homeobox D9	PP
Xl.9560	2.73	9.74×10 ⁻⁴	0.40	5.98×10 ⁻³	<i>Hoxa9</i>	Homeobox A9	PP
Xl.12067	2.80	8.05×10 ⁻³	0.18	2.51×10 ⁻⁵	<i>Esr2</i>	Enhancer of Split related 2	PSM
Xl.29033	2.79	9.31×10 ⁻⁴	0.26	1.62×10 ⁻⁵	<i>Esr9</i>	Enhancer of Split related 9	PSM
Xl.78953	2.90	4.29×10 ⁻⁴	0.37	2.68×10 ⁻³	<i>Tbx6</i>	T-box gene Tbx6	PSM
Xl.483	2.53	4.18×10 ⁻³	0.17	3.36×10 ⁻⁸	<i>Msgn1</i>	Mesogenin 1	PSM
Xl.14524	2.32	2.76×10 ⁻²	0.42	1.46×10 ⁻²	<i>Esr5</i>	Enhancer of Split related 5	PSM
Xl.933	2.49	4.46×10 ⁻²	0.40	2.73×10 ⁻²	<i>xBra3</i>	T2, Brachyury homolog	CNH
Xl.1066	2.44	4.31×10 ⁻²	0.34	2.09×10 ⁻³	<i>xNot</i>	Notochord homeobox	CNH
Xl.457	3.10	1.37×10 ⁻³	0.02	2.81×10 ⁻⁷	<i>Derriere</i>	Growth differentiation factor 3	NC
Xl.16206	2.43	7.64×10 ⁻³	0.27	2.35×10 ⁻⁶	<i>Pnp</i>	Purine nucleoside phosphorylase	NC

Blastula stage embryos were soaked in 1 μ M RAR agonist TTNPB (TTN), 1 μ M RAR inverse agonist AGN193109 (109) or vehicle control (0.1% ethanol) until harvesting at stage 18. Cat, expression category: PP, posterior patterning; PSM, presomitic mesoderm; CNH, chordoneural hinge; NC, expression not characterized. Fold induction or reduction is relative to control vehicle. *P*-values were generated using CyberT.

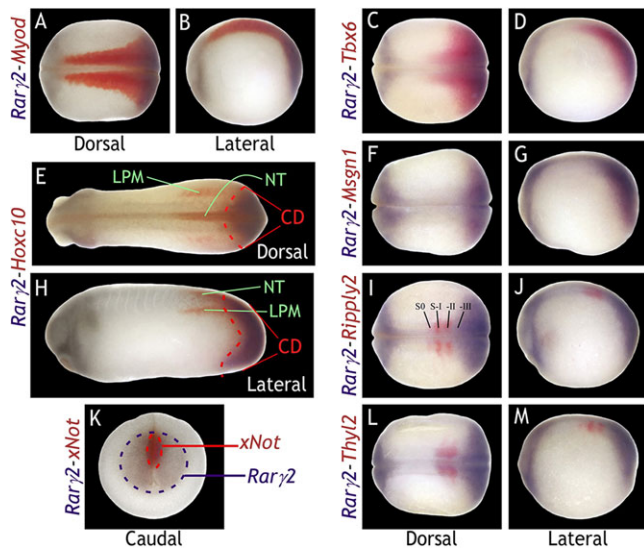


Fig. 1. Double WISH reveals the spatial relationship between *Rary2* and posterior Hox, PSM and CNH genes. (A-M) *Rary2* is stained with BM Purple and the other genes are stained with Fast Red. *Rary2* is caudal to *Myod* and *Tbx6* (A-D), but synexpressed with *Msgn1* (F,G) in neurula stage *Xenopus* embryos. (E,H) *Rary2* is synexpressed with the caudal domain (CD) of *Hoxc10* but not with neural tube (NT) or lateral plate mesoderm (LPM) of *Hoxc10* in tailbud stage embryos. *Rary2* overlaps with S–III domains of *Ripply2* (I,J) and *Thyl2* (L,M) expression, but not with more anterior somitomeres (S–II, S–I, S0). (K) *Rary2* overlaps with *xNot* expression in neurula stage embryos. Dorsal and lateral views shown with anterior to the left, except in K (caudal view with dorsal at top).

Rary2 as a potential regulator of posterior Hox genes and the caudal body plan.

We next defined the anterior limit of *Rary2* expression relative to the determination wavefront. *Myod* is a general muscle marker abutting and partially overlapping *Rary2* expression (Fig. 1A,B). *Thyl2* and *Ripply2* mark somitomeres, which are prepatterned PSM domains containing non-epithelialized, immature somites (Tam et al., 2000). *Thyl2* and *Ripply2* are only expressed in newly forming somitomeres and are assigned negative Roman numerals (S–I, S–II, etc.) versus mature somites (SI, SII, etc.) (Pourquie and Tam, 2001). *Msgn1* (Buchberger et al., 2000) is expressed caudal to *Thyl2* and *Ripply2*, marking non-patterned PSM-containing cells committed to the somitic fate (Nowotschin et al., 2012). *Tbx6* is also expressed in PSM, but unlike *Msgn1* its expression domain overlaps with somitomeres (Hitachi et al., 2008). *Rary2* and *Msgn1* are synexpressed at neurula (Fig. 1F,G) and tailbud (supplementary material Fig. S3) stages; *Tbx6* expression overlaps *Rary2* but extends rostrally beyond the *Rary2* domain (Fig. 1C,D; supplementary material Fig. S3). Anterior expression of *Rary2* mRNA ends at an RA-responsive region (supplementary material Fig. S4), coinciding with the most posterior somitomere domain (S–III) of *Thyl2* or *Ripply2* (Fig. 1I–M), thus skirting the posterior edge of the wavefront.

xNot, a notochord marker that regulates trunk and tail development, is concentrated in the extreme posterior notochord and floor plate by late neurula (von Dassow et al., 1993) and is often employed as a CNH marker in *Xenopus* (Beck and Slack, 1998) to reveal the location of bipotential stem cells (Cambray and Wilson, 2007; Takemoto et al., 2011). *xNot* is co-expressed with *Rary2* (Fig. 1K), agreeing with data suggesting that *Rary2* is present in CNH (Pfeffer and De Robertis, 1994). The double WISH data are consistent with *Rary2* functioning as an activator near where RA is

present at the wavefront, yet as a repressor where it coincides with *Msgn1*, *xNot* and *Cyp26a1*.

RAR γ -selective chemicals modulate activation or repression by RAR γ

To separate the effects of RAR γ in the posterior from RAR α in the trunk, we characterized RAR γ -selective agonist NRX204647 (4647) (Shimono et al., 2011; Thacher et al., 2000) and RAR γ -selective inverse agonist NRX205099 (5099) (Tsang et al., 2003) in *Xenopus* embryos. Like AGN193109, 5099 is an inverse agonist, reducing RAR γ signaling activity below basal levels by stabilizing the co-repressor complex bound to RAR γ . Embryos treated with 1 μ M agonist 4647 become primarily trunk (no head or tail structure), while 0.1 μ M perturbs axial elongation (supplementary material Fig. S5), producing anterior truncations characteristic of RAR activators (Sive et al., 1990). Inverse agonist 5099 at 1 μ M delayed development, producing enlarged heads and shortened trunks; half the dose elicited similar but weaker phenotypes, with effects absent at 0.1 μ M (supplementary material Fig. S5). Treating neurula embryos significantly reduced severity but did not eliminate the phenotype (supplementary material Fig. S5).

To test the effects of these chemicals *in vivo* without interference from endogenous RARs, we mutated the DNA-binding specificity of a full-length RAR, RAR^{EGCKG→GSKKV}. The mutant receptor recognizes a mutant TK-luc reporter, (RXRE^{1/2}-GRE^{1/2}) \times 4 TK-luc, to which endogenous RARs do not bind (Klein et al., 1996). In transient transfection assays, 4647 selectively activated RAR γ at doses below 0.1 μ M (supplementary material Fig. S6A). Similarly, 5099 selectively antagonized 10 nM 9-cis RA activation of RAR γ below 0.1 μ M (supplementary material Fig. S6B). We conclude that 4647 and 5099 behave as subtype-selective ligands to activate or repress RAR γ .

RAR γ -selective chemicals affect posterior Hox genes, PSM and somitomeres

We hypothesized that 4647 treatment of embryos would decrease posterior Hox gene expression and markers of PSM, whereas 5099 would produce the opposite effect. Microarray analysis (Table 1) revealed that *Hoxc13* and *Hoxc10* expression was upregulated by inverse agonist AGN193109 and downregulated by agonist TTNPB. We infer that increased expression of *Hoxc13* and *Hoxc10* results from RAR repressing the expression of a repressor of their expression. The expression pattern of *Hoxc13* (supplementary material Fig. S7) was not previously characterized.

We began soaking embryos in RAR γ -selective doses of 4647, 5099 or vehicle control after gastrulation (stage 12.5) to focus on axial elongation. Treatment with 10 nM 4647 resulted in diminished caudal structures at stage 40 (supplementary material Fig. S5), reducing expression domains of *Hoxc10*, *Hoxd10* and *Hoxc13* (Fig. 2A–C). Conversely, treatment with 0.5 μ M 5099 expanded their neural and lateral domains (Fig. 2A–C). To determine short-term effects of chemical treatments, we soaked embryos for 1 h at various stages and evaluated *Hoxc10* expression (supplementary material Fig. S8) and that of *Tbx6* (not shown) at stage 22. Repression by 5099 is required at early neurula, whereas activation by 4647 is required at mid- and late neurula stages for expected expansion and reduction, respectively, of *Hoxc10* expression (supplementary material Fig. S8). Higher, non-receptor-selective doses exacerbated effects on posterior Hox genes (supplementary material Fig. S9), suggesting that RAR γ 2 is the primary mediator. *Hoxc10* nearly abuts *Krox20*, demonstrating trunk shortening in 5099-treated embryos (supplementary material Fig. S9G,H). High

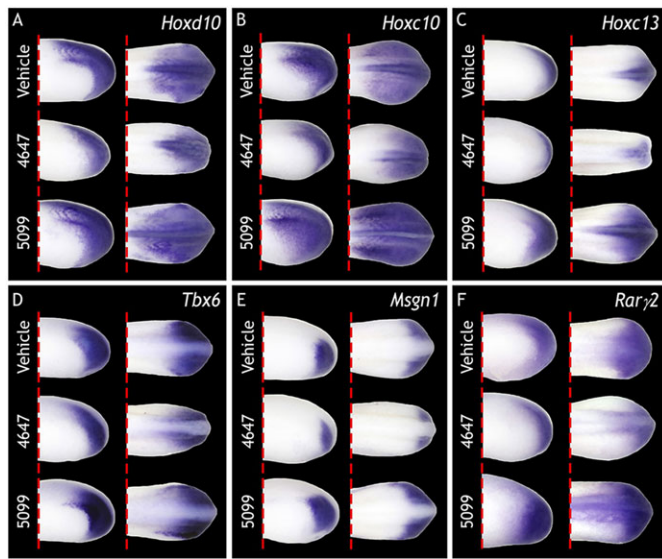


Fig. 2. Posterior Hox and PSM markers are reduced by RAR γ -selective agonist and expanded by RAR γ -selective inverse agonist. (A-F) WISH from embryos treated post-gastrulation (stage 12.5) with 10 nM 4647, 0.5 μ M 5099 or vehicle (0.1% ethanol). Dashed red line represents half the embryo axis. 4647 diminishes and 5099 expands the expression of (A) *Hoxd10* (4647, 16/16; 5099, 17/17 embryos), (B) *Hoxc10* (4647, 14/14; 5099, 21/21), (C) *Hoxc13* (4647, 12/12; 5099, 16/16), (D) *Tbx6* (4647, 11/12; 5099, 17/17), (E) *Msgn1* (4647, 15/15; 5099, 14/14), and (F) *Rary2* (4647, 15/15; 5099, 9/9) relative to control vehicle. Embryos shown in lateral or dorsal view at tailbud stage, anterior to left.

doses of 4647 create embryos lacking anterior and posterior structures, as indicated by the absence of mid/hindbrain markers *En2* and *Krox20* and of posterior gene *Hoxc10* (supplementary material Fig. S9C-F).

Msgn1 and *Tbx6* were upregulated by inverse agonist and downregulated by agonist in the microarray analysis (Table 1). *Msgn1* and *Tbx6* domains were reduced at tailbud stages by post-gastrulation treatment of embryos with 4647, whereas expression was expanded in embryos treated with inverse agonist 5099 (Fig. 2D,E). However, in neurula stage embryos, 4647 reduced *Msgn1* expression while *Tbx6* expression was expanded (Fig. 3E,F,O,P). Expression of *Tbx6* and *Msgn1* was expanded by 5099 (Fig. 3I,J,Q,R), an effect that was more pronounced at higher doses (supplementary material Fig. S10I,J,Q,R). Somitomere markers *Thyl2* and *Ripply2* showed thicker domains; S–III expanded to the posteriormost edge of the embryo where somites are not found in controls (Fig. 3G,H). At non-receptor-selective doses, 4647 exacerbated the phenotypes of *Msgn1*, *Tbx6* and *Ripply2* (supplementary material Fig. S10E,F,H,O,P) and promoted ectopic expression of *Thyl2* in the midline, with somitomeres occupying nearly the entire anteroposterior axis (supplementary material Fig. S10G). By contrast, 5099 treatment produced fewer, thinner somitomeres (Fig. 3K,L), an effect more pronounced at higher doses (supplementary material Fig. S10K,L).

Since *Rary2* is co-expressed with *Msgn1*, we expected that 4647 would reduce and 5099 would expand *Rary2* expression. *Rary2* expression was expanded by inverse agonist and reduced by agonist (Fig. 2F) as verified by QPCR (supplementary material Fig. S11), which is surprising given that other receptor subtypes (RAR α 2 and RAR β 2) are induced by agonist (Leroy et al., 1991; Sucov et al., 1990). The data indicate that 5099 enhances repression by RAR γ , increasing caudal gene expression, whereas 4647 relieves repression by RAR γ , diminishing caudal gene expression.

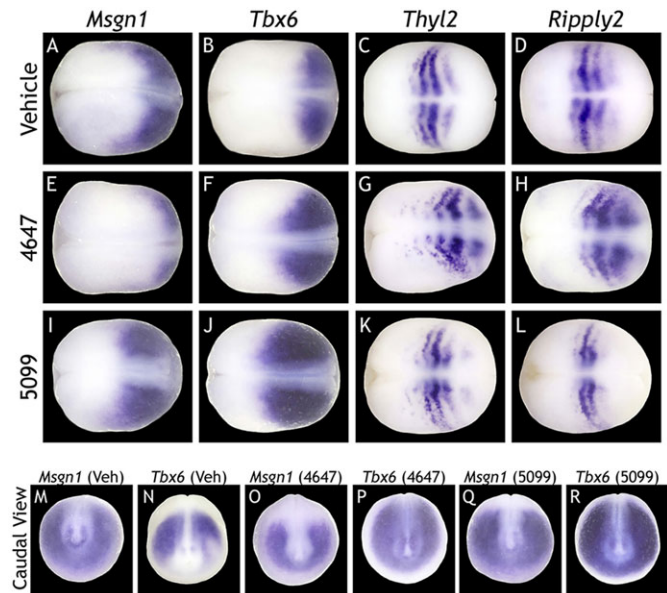


Fig. 3. PSM markers are modulated by RAR γ -selective agonist and inverse agonist. (A-R) WISH from embryos treated post-gastrulation (stage 12.5) with 10 nM 4647, 0.5 μ M 5099 or vehicle (0.1% ethanol). (A-D) Control expression of *Msgn1*, *Tbx6*, *Thyl2* and *Ripply2*. (E) *Msgn1* expression diminished by 4647 treatment (17/17 embryos). (F) *Tbx6* expression expanded by 4647 treatment (22/22). (G,H) Somitomere domains of *Thyl2* (19/19) and *Ripply2* (17/17) are thicker and posteriorly expanded. (I,J) *Msgn1* (17/17) and *Tbx6* (13/13) expression expanded by 5099 treatment. (K,L) Somitomere domains of *Thyl2* (15/17) and *Ripply2* (26/26) are fewer and thinner. Embryos are shown in dorsal view at neurula stage, anterior to left. (M-R) Caudal views of *Msgn1* and *Tbx6*.

Relief of repression reduces domains of posterior Hox and PSM markers

Treatment with 4647 activates RAR γ and removes repressors from RAR γ targets, creating posterior truncations. We hypothesized that loss of RAR γ 2 would phenocopy 4647 treatment once RAR γ 2-mediated repression was lost. We designed AUG MOs to capture both pseudoalleles of *Rary2*. Knockdown of RAR γ 2.1/2.2 resulted in loss of *Hoxc10*, *Hoxd10*, *Hoxa11* and *Hoxc13* expression, with severe curvature and reduction of the injected side (Fig. 4A-D). Microinjection of splice-blocking MO capturing both pseudoalleles of *Rary2* reduced the expression of *Rary2* as measured by QPCR, phenocopying the AUG MOs (supplementary material Fig. S12). We demonstrated that axial truncation on the injected side was not due to developmental delay (supplementary material Fig. S13). To establish that RAR γ 2 is solely responsible for the axial truncations and reduction in posterior Hox and PSM domains, we showed that *Rary2* MO can only be rescued with *Rary2*, but not *Rara2* or *Rar β 2*, mRNA (Fig. 5). RAR γ 2 knockdown reduced and shifted the expression of *Msgn1* and *Tbx6* anteriorly along the midline (Fig. 4E,F,I-J') and caused an anterior shift in the paraxial domains of *Thyl2* and *Ripply2*, while obliterating lateral expression (Fig. 4G,H). The complexity of the *Rary2* MO phenotype is likely to be due to the fact that RAR γ 2 knockdown both disrupts its repressive function in the absence of ligand and its activation in the presence of ligand, particularly near the determination wavefront.

When the dominant-negative co-repressor c-SMRT is overexpressed, it binds RAR and blocks recruitment of co-repressors (Chen et al., 1996). We identified several c-SMRT isoforms from *Xenopus*, selecting that most similar to human c-SMRT that we used previously. Microinjection of *Xenopus laevis* (Xl) *c-smrt* mRNA relieved

repression by GAL4-xRAR γ in whole embryos (supplementary material Fig. S14). This effect was potentiated by addition of 1 μ M TTNPB (supplementary material Fig. S14). Overexpression of XI *c-smrt* mRNA caused significant reductions in the neural and lateral domains of *Hoxc10* and *Hoxd10* (Fig. 6B,D). XI *c-smrt* also reduced *Hoxc13*, *Tbx6*, *Msgn1* and *xNot* (Fig. 6F,H,H',J,J',L). Similar to *Rary2* MO, moderate truncation of injected axes was observed in 70% of embryos, but the midline, rostral shifting of *Tbx6* and *Msgn1* (as in *Rary2* MO embryos) was minimal. We conclude that XI *c*-SMRT relieves repression of *Rary2*, causing loss of progenitor and PSM cells and posterior Hox gene expression.

Another method for relieving repression is overexpression of constitutively active VP16-RAR γ 2 (RAR γ 2 fused to the VP16 activation domain). Microinjection of VP16-*Rary2* mRNA led to a truncated axis on the injected side in 100% of embryos and loss of *Hoxc10*, *Hoxd10*, *Msgn1* and *Tbx6* expression (Fig. 7). These embryos were less curved than *Rary2* MO-injected or *c-smrt*-injected embryos, but rostral expansion of neural/midline and lateral domains was consistently observed, similar to *Rary2* MO embryos.

Increased repression expands posterior Hox and PSM markers

Treatment with 4647 or microinjection of *c-smrt* or VP16-*Rary2* mRNA relieved repression by RAR γ , increasing RAR signaling, decreasing posterior Hox and PSM markers. Decreasing RAR signaling should produce the opposite effect. We microinjected mRNA overexpressing the RA catabolic enzyme CYP26A1 and observed rostral shifts in the lateral and neural expression domains of *Hoxc10* and *Hoxd10* (supplementary material Fig. S15). Microinjection of dominant-negative (DN)-RAR γ 2 should phenocopy 5099 treatment because co-repressors would be retained on RAR γ 2 targets, leading to repression. Overexpression of DN-RAR γ 2 increased the expression of *Msgn1* and *Tbx6* in both lateral and paraxial domains, and shifted *xNot* expression rostrally

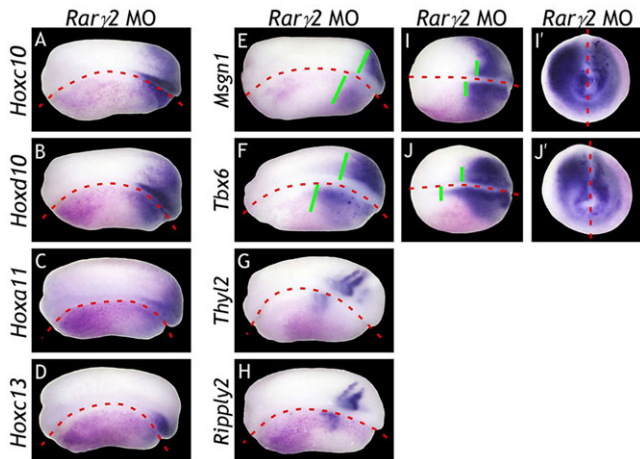


Fig. 4. RAR γ 2 knockdown alters expression of posterior Hox and PSM markers. (A-J') Embryos were injected unilaterally at the 2- or 4-cell stage with 7.5 ng *Rary2.1* MO+7.5 ng *Rary2.2* MO. Injected side is indicated by magenta β -gal lineage tracer. *Rary2.1/2.2* MO decreases expression of (A) *Hoxc10* (18/18 embryos), (B) *Hoxd10* (12/12), (C) *Hoxa11* (9/9) and (D) *Hoxc13* (16/16) in tailbud stage embryos. *Rary2.1/2.2* MO decreases lateral, but expands midline, expression (green lines) of (E) *Msn1* (10/13) and (F) *Tbx6* (8/11), knocking down and shifting expression rostrally of (G) *Thy12* (13/15) and (H) *Ripply2* (13/14) in tailbud stage embryos. *Rary2.1/2.2* MO decreases lateral, but expands midline, expression (green lines) of (I) *Msn1* (35/36) and (J) *Tbx6* (20/20) in neurula stage embryos. Embryos shown in dorsal view with anterior on left. (I', J') Caudal views of I and J.

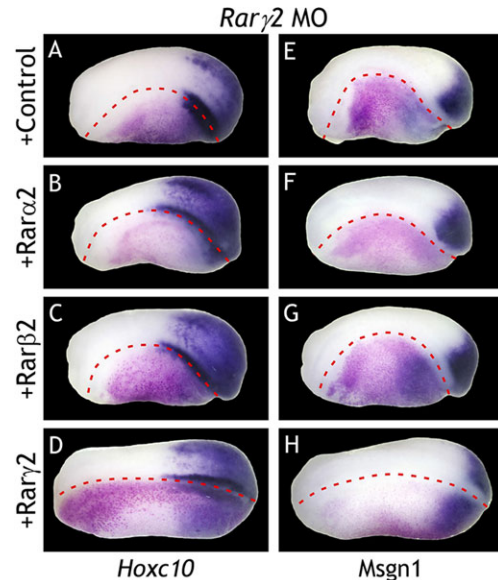


Fig. 5. *Rary2* mRNA rescues posterior Hox and PSM expression in *Rary2* MO embryos. (A-H) Embryos injected unilaterally at 2- or 4-cell stage. Injected side is indicated by magenta β -gal lineage tracer. (A,E) 5 ng *Rary2.1* MO+5 ng *Rary2.2* MO+control (*mCherry*) mRNA diminishes *Hoxc10* and *Msn1* expression, curving the embryo axis in 100% of embryos (*Hoxc10*, 23/23; *Msn1*, 13/13). (B,C,F,G) Co-injection of *Rary2* MO and 1 ng *Rara2* mRNA or 1 ng *Rarβ2* does not rescue the phenotype; however, (D,H) 1 ng *Rary2* mRNA partially rescues axial curvature and *Hoxc10* (18/23) and *Msn1* (23/35) expression. Tailbud embryos shown in dorsal view with anterior to left.

(Fig. 8B,D,F). DN-RAR γ 2 phenocopied the effects of *Cyp26a1* mRNA (Moreno and Kintner, 2004) on somitomere markers *Thyl2* and *Ripply2*; rostral shifting and knockdown of somitomere expression was the phenotype that we observed (Fig. 8H,J,K).

Microinjection of *Rary2* MO alone resulted in knockdown of *Hoxc10* and axial truncation (Fig. 9A,B,E). We hypothesized that this phenotype was due to loss of repression, reasoning that the phenotype should be rescued with DN-RAR γ 2. Axial defects and lateral knockdown of *Hoxc10* expression were partially recovered with DN-*Rary2* mRNA (Fig. 9C,D,E). The neural domain of *Hoxc10* expression was rescued in nearly all embryos and a rostral shift often observed. We conclude that increasing repression with DN-RAR γ 2 or overexpressing CYP26A1 (removing ligand) promotes caudal gene expression, similar to chemical treatment with 5099. Moreover, loss of caudal structures and gene expression due to *Rary2* MO are rescued by restoring repression with DN-RAR γ 2.

DISCUSSION

RAR γ repression in caudal development

Most studies consider only one aspect of RAR signaling, namely its role as a ligand-activated transcription factor promoting the expression of target genes. In developmental biology, RA signaling has been studied extensively for its ability to promote differentiation and establish boundaries in somitogenesis, neurogenesis and rhombomere segmentation (reviewed by Rhinn and Dolle, 2012). Liganded RAR has been predicted to function passively in the caudal region until required to facilitate body axis cessation (Olivera-Martinez et al., 2012), when somitogenesis is nearing completion because the determination wavefront, moving the RA source caudally, has exhausted the progenitor cell pool (Gomez and Pourquie, 2009). Here, liganded RAR γ would function as an activator promoting apoptosis (Shum et al., 1999) at terminal tailbud stage. However, this does not address why RAR γ 2 would be highly expressed where RA is

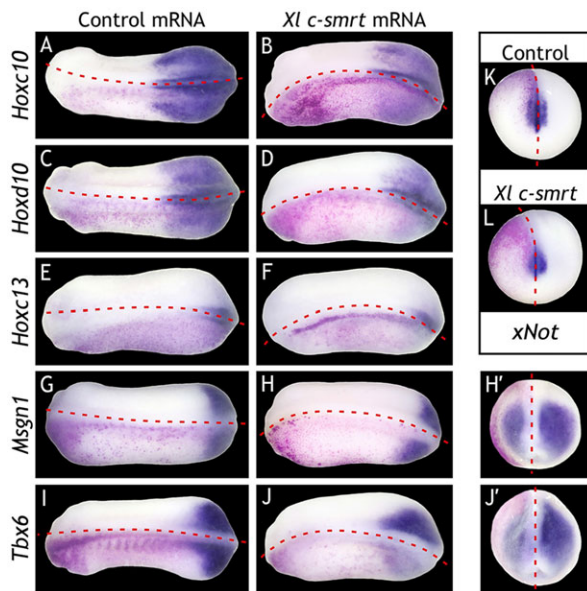


Fig. 6. c-SMRT overexpression knocks down posterior Hox, PSM and CNH markers. Embryos injected unilaterally at 2- or 4-cell stage with 4 ng *c-smrt* mRNA or control (*mCherry*) mRNA. Injected side indicated by magenta β -gal lineage tracer. (A,C,E,G,I,K) Control expression of *Hoxc10*, *Hoxd10*, *Hoxc13*, *Msgn1*, *Tbx6* and *xNot*. (B,D,F,H,J,L) *c-smrt* overexpression shortens the axis on injected side in 70% of embryos. (B) *c-smrt* mRNA results in lateral knockdown (13/23 embryos), neural knockdown (7/23) or neural rostral shift (7/23) in *Hoxc10* expression. (D) *c-smrt* mRNA produces neural and lateral knockdown (15/19) or lateral knockdown alone (4/19) of *Hoxd10* expression. (F,H,J) *c-smrt* mRNA knocks down expression of *Hoxc13* (14/18), *Msgn1* (12/14) and *Tbx6* (15/15). Tailbud embryos shown with anterior to left. (H',J') Caudal views of H and J. (L) *c-smrt* mRNA knocks down *xNot* (12/15) expression in neurula stage embryos (caudal view, dorsal to top).

presumed absent due to CYP26A1 expression. Here we show that RAR γ is engaged in all stages of caudal development, not solely as a terminator of the body axis. RAR γ functions as an unliganded repressor required for the maintenance of the posterior PSM and progenitor cell population that allows axial elongation (Fig. 10). RAR γ acts as a liganded activator in the anterior, segmented PSM to facilitate somite differentiation (Fig. 10). Repression mediated by the unliganded receptor-co-repressor complex constitutes a novel mechanism by which posterior markers are upregulated during axial elongation in *Xenopus* embryos.

Our microarray results suggest that axial elongation is regulated by RAR-mediated repression. Enhancing repression with AGN193109 upregulated, and activation of RAR by TTNPB downregulated, many posterior Hox, PSM and CNH genes in neurula stage embryos. We identified AGN193109-upregulated genes expressed in PSM (Table 1) that are mostly absent from regions of somite maturation (Blewitt, 2009; Yoon et al., 2000). The CNH markers *xBra3* and *xNot* were also upregulated by AGN193109, thus both PSM and CNH markers were upregulated by enhancing RAR repression and downregulated by increasing RAR activation. Current literature suggests the existence of a negative-feedback loop between these two populations of cells: *Msgn1* is induced by *Brachyury* and *Wnt8* in CNH but represses their expression to promote PSM fates (Fior et al., 2012; Yabe and Takada, 2012). Our results support a novel role of RAR repression in the maintenance of cells in both unsegmented PSM and stem-like CNH.

We showed that *X. laevis* RAR α , RAR β and RAR γ can repress basal transcriptional activity in the absence of RA and examined whether this repression is physiologically relevant in caudal

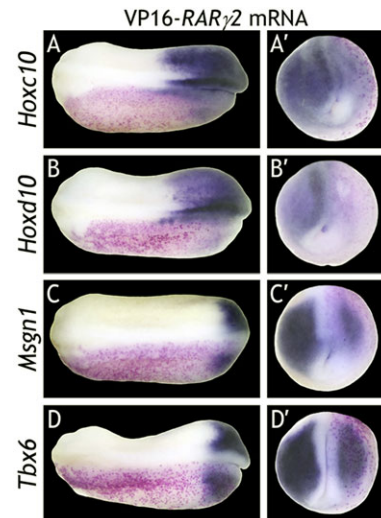


Fig. 7. VP16-RAR γ 2 overexpression knocks down posterior Hox and PSM marker expression. Embryos injected unilaterally at 2- or 4-cell stage with 0.3 ng VP16-*Rary2* mRNA or control (*mCherry*) mRNA. Injected side is indicated by magenta β -gal lineage tracer. Control expression of *Hoxc10*, *Hoxd10*, *Msgn1* and *Tbx6* is shown in Fig. 6A,C,G,I. (A-D) VP16-*Rary2* overexpression shortens the axis on injected side in 100% of embryos. (A,B) VP16-*Rary2* mRNA results in neural/midline rostral shift and lateral knockdown in *Hoxc10* (9/13 embryos) and *Hoxd10* (7/13) expression. Neural/midline knockdown is also observed (*Hoxc10*, 4/13; *Hoxd10*, 7/13). (C,D) VP16-*Rary2* mRNA rostrally shifts and/or knocks down *Msgn1* (12/12) and *Tbx6* (13/13) expression. Tailbud embryos shown with anterior to left. (A'-D') Caudal views of A-D.

development. *Rary2* is expressed in embryonic regions where it might actively repress genes involved in axial elongation. *Rary2* is synexpressed with the PSM marker *Msgn1* and overlaps with *Tbx6*, *Hoxc10*, the S-III domains of *Thyl2* and *Ripply2*, and the CNH marker *xNot*. By contrast, *Rary2* is expressed at low levels in trunk (where *Myod* and *Rar α* are expressed) and in the anterior, segmented PSM expression domains of *Thyl2* and *Ripply2*. Since absence of RA is required for the proliferation and/or survival of caudal PSM and CNH cells, the presence of RAR γ in posterior tissue would be contradictory if it functioned as an activator. We infer that RAR γ acts as a repressor throughout unsegmented PSM and CNH where RA is absent, but as an activator of somitomere markers near the differentiation wavefront where *Rary2* overlaps with S-III and where *Raldh2* expression indicates the presence of RA. It remains unknown what repressors RAR γ targets to indirectly upregulate caudal genes. One possibility is that RAR γ represses *Ripply2*, which functions to repress *Tbx6* (reviewed by Dahmann et al., 2011), as supported by the observation that increasing activation with 4647 expands *Ripply2* posteriorly. Hence, RAR γ would normally function in the posterior to repress *Ripply2*, therefore promoting expression of *Tbx6*.

RAR γ repression promotes the maintenance of unsegmented PSM and CNH

Since high doses of 4647 result in embryos consisting largely of trunk, it is predictable that nearly the entire embryo differentiated into somitomeres (with thicker boundaries). At lower, RAR γ -selective 4647 doses, somitomeres were shifted posteriorly and thickened. This phenotype, which is also seen with RA treatment or FGF inhibition by SU5402, was attributed to increased numbers of cells allocated to somitomeres and a decreased progenitor pool (Dubrulle et al., 2001; Moreno and Kintner, 2004). 5099 upregulates both *Tbx6* and *Msgn1*, indicating that unsegmented PSM is expanded by increased RAR

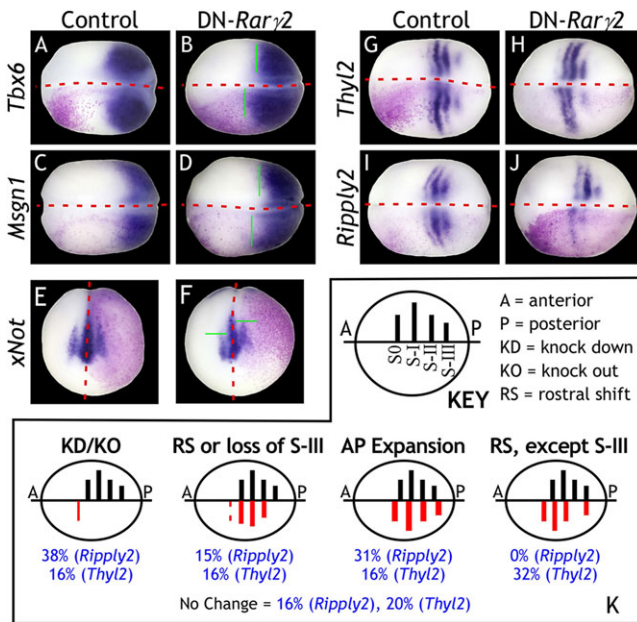


Fig. 8. Overexpression of DN-*Rar* γ 2 mRNA expands expression of PSM and CNH markers, shifting or knocking down somitome markers *Thy12* and *Ripply2*. (A-J) Embryos injected unilaterally at 2- or 4-cell stage. Injected side is indicated by magenta β -gal lineage tracer. (A,C,E,G,I) Control (*mCherry*) mRNA does not alter expression of *Tbx6*, *Msgn1*, *Thy12*, *Ripply2* or *xNot*. (B,D,F) 2 ng DN-*Rar* γ 2 mRNA expands expression of *Msgn1* (8/11) and *Tbx6* (15/23) (green lines) and rostrally shifts *xNot* (8/10). (H,J) DN-*Rar* γ 2 overexpression produces multiple phenotypes of *Thy12* and *Ripply2* expression, as characterized and scored in K. Neurula embryos shown in dorsal view with anterior to left.

repression. However, we note distinct differences in the effects of 4647 on *Tbx6* versus *Msgn1*. *Tbx6* is upregulated by 4647 at early stages but downregulated at later stages, as also observed for the T-box gene *Tbx1* (Janesick et al., 2012). Unlike *Msgn1*, *Tbx6* plays a dual role in the unsegmented PSM and the determination front where it controls the anteroposterior patterning of somitomes via *Ripply2* (Hitachi et al., 2008).

Msgn1 expression does not overlap somitomes and functions to maintain unsegmented PSM by encouraging the differentiation of caudal stem cells. Loss of *Msgn1* expression leads to smaller somitomes owing to the accumulation of bipotential progenitor cells that have not received signals to commit to PSM fate (Fior et al., 2012; Yabe and Takada, 2012). Treatment with 4647 also leads to loss of *Msgn1* and thus somitomes should be smaller; however, they are larger. Despite such divergent early stage phenotypes, *Msgn1*^{-/-} embryos (Yoon and Wold, 2000) and 4647 embryos both display fewer somites and reduced caudal structures at late stages. Caudal progenitors cannot be instructed to become somites in *Msgn1*^{-/-} embryos. In 4647-treated embryos, the pool is expeditiously transformed into thickened somitomes early, but the progenitor supply is exhausted before axial elongation is complete, reducing somitome numbers. That 4647 can differentiate somitomes at all without *Msgn1* is intriguing. Either *Tbx6* compensates for *Msgn1* knockdown, or 4647 can induce uncommitted, non-PSM progenitor cells to differentiate into somitomes.

Relief of RAR γ repression suppresses PSM and CNH marker gene expression

If RAR γ functions solely as a repressor, then RAR γ knockdown should induce a loss of repression phenotype. *Rary2* MO

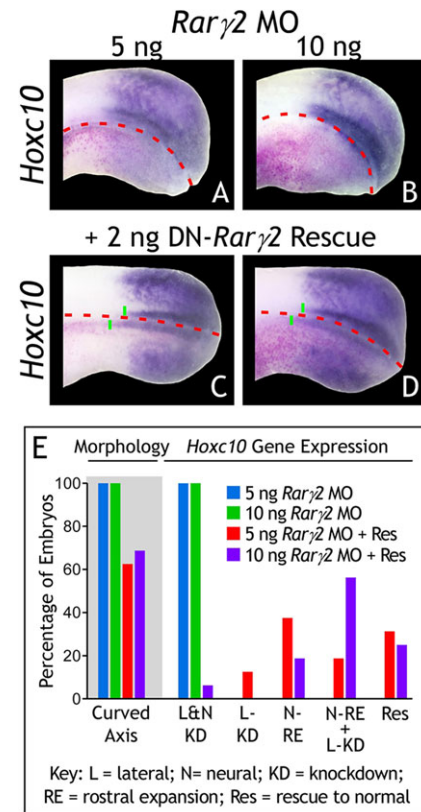


Fig. 9. DN-*Rar* γ 2 mRNA rescues posterior *Hoxc10* expression in *Rary2* MO embryos. (A-D) Embryos injected unilaterally at 2- or 4-cell stage. Injected side is indicated by magenta β -gal lineage tracer. (A) 2.5 ng *Rary2.1* MO + 2.5 ng *Rary2.2* MO or (B) 5 ng *Rary2.1* MO + 5 ng *Rary2.2* MO diminishes *Hoxc10* expression and curves the embryo axis. (C,D) 2 ng DN-*Rar* γ 2 mRNA partially rescues this effect and expands neural expression of *Hoxc10*. Tailbud embryos shown in dorsal view with anterior to left. (E) Detailed scoring of the rescue experiment.

microinjection resulted in severely truncated body axes with caudal PSM and posterior *Hox* markers significantly reduced at tailbud stages, similar to 4647 treatment. This phenotype was attributed to axial defects, not merely developmental delay. We noted three differences between 4647-treated and *Rary2* MO-injected embryos. First, axes of *Rary2* MO embryos were significantly curved, which was attributed to imbalance/dominance of the uninjected side versus the truncated injected side. Second, caudal PSM markers, while qualitatively reduced with *Rary2* MO, also expanded rostrally, even when accounting for shortened axes on injected sides. Third, thickened, posteriorly expanded somitomes were not seen with *Rary2* MO. RAR γ acting as an activator near the somitogenesis front where RA is present would explain some discrepancies. RA functions in the determination wavefront to antagonize proliferating PSM and promote somitome differentiation (Moreno and Kintner, 2004). If RA acts through RAR γ in the wavefront, then loss of *Rary2* should expand unsegmented PSM and reduce somitome expression, exactly as observed.

Axial curvature and loss of *Hoxc10* and *Msgn1* expression in *Rary2* MO-injected embryos could be rescued by *Rary2*, but not *Rara2* or *Rarb2* mRNA. Therefore, *Rary2* is the sole receptor responsible for axial elongation, in agreement with *Rary2* as the only RAR expressed in caudal domains. *Rarb2* is present only in trunk and pharyngeal arches (Escriva et al., 2006) and *Rara2* is completely absent from the blastopore and surrounding area (see figure S1A,B in the supplementary material of Janesick et al.,

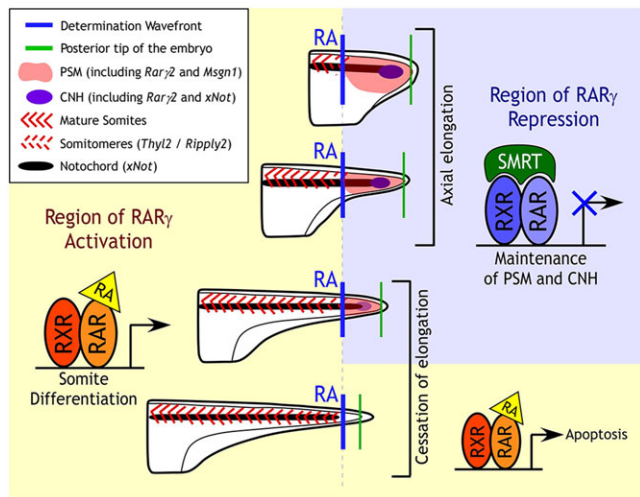


Fig. 10. RAR γ functions as both transcriptional activator and repressor during somitogenesis and axial elongation. RAR γ is activated by RA near the determination wavefront where PSM differentiates into somitomeres, then mature somites. The progenitor pool within the PSM and CNH domains, which is maintained by RAR γ repression, feeds into the wavefront until exhausted, as somitogenesis proceeds faster than progenitors are replenished (Gomez and Pourquie, 2009). As PSM and CNH domains diminish, the distance between RA/wavefront (blue line) and the posterior tip of the embryo (green line) becomes shorter. RA is able to enter the posterior, activating RAR γ , switching its function from repressor promoting growth to activator terminating growth. RXR, retinoid X receptor.

2013). *Hoxc10* expression could be rescued in *Rary2* MO-injected embryos by co-injecting DN-*Rary2* mRNA, definitively establishing that RAR γ 2 functions as a repressor in the caudal domain. DN-RAR γ 2 restored *Hoxc10* expression, especially in neural tube, where additional rostral expansion was often observed. DN-RAR γ 2 rescue restored curved axes only partially. We predict that axial curvature is a loss-of-activation effect inhibiting somitomere formation; therefore, the phenotype should not be rescued by DN-RAR γ 2, but rescued by wild-type RAR γ 2, as we observed.

Perhaps the most direct method for relieving repression of RAR γ 2 in caudal regions is overexpression of dominant-negative co-repressor c-SMRT, which binds RAR γ 2 preventing recruitment of co-repressors and thereby blocking repression. c-SMRT overexpression resulted in truncated axes with loss of posterior Hox, unsegmented PSM and CNH markers, but not rostral shifting of *Msgn1* and *Tbx6* as had been observed for *Rary2* MO embryos. This indicates that rostral shifting in *Rary2* MO embryos results from loss of activation rather than relief of repression. We previously showed that c-SMRT not only relieves repression of RAR but also potentiates ligand-mediated activation (Koide et al., 2001). Since c-SMRT was expressed ubiquitously, it could superactivate RAR α or RAR γ where RA is present. It should also be noted that c-SMRT can interact with other nuclear receptors and transcription factors. Therefore, we can only conclude that c-SMRT overexpression inhibits maintenance of the caudal PSM and progenitor pool (where RA is absent). We cannot draw conclusions about somitomere markers in c-SMRT overexpression embryos since their expression is controlled by RAR activation, which c-SMRT does not reduce.

RAR signaling and posterior Hox gene regulation

We identified a novel function for RAR γ as a transcriptional repressor in the regulation of posterior Hox genes. Posterior Hox genes pattern

caudal embryonic regions, promote axial elongation (Young et al., 2009) and are linked to cell cycle progression (Gabellini et al., 2003) and therefore proliferation. Axial elongation involves the addition of tissue, as cells must proliferate to contribute segments. Normally, FGF and RA signaling are mutually antagonistic, but we provide evidence that RAR γ can support proliferative mechanisms in the absence of RA.

Hox gene expression was altered by 4647 and 5099 treatment, even post-gastrulation. Hence, although Hox gene expression is initiated collinearly during gastrulation, this temporal pattern is not immutable. In support of this model, axial progenitor cells transplanted to anterior locations do not retain their previous Hox identity (McGrew et al., 2008). Furthermore, manipulation of anteroposterior locations of PSM and the determination wavefront resulted in corresponding changes in Hox gene expression (Iimura et al., 2009; Wellik, 2007). We showed that 4647 treatment pushes determination fronts caudally and observed posterior regressions of *Hoxc10*, *Hoxd10* and *Hoxc13* expression. Conversely, rostral expansion in PSM by increasing RAR repression was accompanied by anterior shifts in posterior Hox expression. Owing to posterior prevalence, rostral shifts of *Hoxc10* or *Hoxd10* expression could indicate that thoracic segments will develop caudal structures at later stages. Similarly, rostral shifts in *Hoxc13* could drive lumbar segments to sacral morphology. Homeotic transformations from manipulating RAR repression deserve future study.

Conclusions

We conclude that the RAR-mediated repression of caudal genes is crucial for axial elongation, establishing another important role for active repression by nuclear receptors in body axis extension, as previously shown for head formation (Koide et al., 2001). RAR γ 2 is likely to function as an activator near the determination wavefront and a repressor to maintain axial progenitor pools in the PSM and CNH. As axial elongation nears completion, RAR γ 2 functions as an activator because the progenitor pool is exhausted and RA comes into close proximity to the caudal domain of RAR γ 2, where it can then promote apoptosis and terminate the body axis. This model is attractive because it utilizes the same protein to activate or repress target genes depending on the proximity to RA and explains the high levels of posterior RAR γ 2 expression. RAR γ 2 is likely to function in multiple steps of somitogenesis and axial elongation (Fig. 10): (1) preservation of undifferentiated states in the progenitor pools (marked by the CNH); (2) maintenance of PSM; (3) initiation of somitomere differentiation; and (4) axial termination. Future studies require RAR γ target gene identification because very few ChIP studies have ascertained direct targets, and even fewer studies have explored subtype-selective RAR targets. In the case of inverse agonist-upregulated genes (the focal point of our study), identifying repressors of PSM and progenitors will be key, as these genes are likely to be targeted by unliganded RAR in a classic 'repression of a repressor' mechanism.

MATERIALS AND METHODS

Percellome microarray analysis

Xenopus laevis eggs from three different females were fertilized *in vitro* and embryos staged as described (Janesick et al., 2012). Stage 7 embryos were treated in groups of 25 in 60-mm Petri dishes with 10 ml 0.1 \times MBS containing 1 μ M RAR agonist (TTNPB), 1 μ M RAR inverse agonist (AGN193109) or vehicle control (0.1% ethanol). Three dishes per treatment per female were collected (27 dishes total: three technical replicates, three biological replicates per treatment). Each dish of embryos was harvested at stage 18 into 1.5 ml RNAlater (Invitrogen) and stored at 4°C. Samples were homogenized, RNA isolated and DNA quantitated (Kanno et al., 2006). Graded-dose spiked cocktail

(GSC) made of five *Bacillus subtilis* RNA sequences present on Affymetrix GeneChip arrays (AFFX-ThrX-3_at, AFFX-LysX-3_at, AFFX-PheX-3_at, AFFX-DapX-3_at, AFFX-TrpX-3_at) was added to the sample homogenates in proportion to their DNA concentration (Kanno et al., 2006). GSC-spiked sample homogenates were processed and probes synthesized using standard Affymetrix protocols, applied to *Xenopus* microarray v1.0 GeneChips and analyzed using Perccellome software (Kanno et al., 2006). Absolutized mRNA levels were expressed as copy number per cell for each probe set.

Perccellome microarray data were analyzed using CyberT (Kayala and Baldi, 2012). We did not use low value thresholding/offsetting or log/VSN normalizations. Bayesian analysis used a sliding window of 101 and confidence value of 10. The *P*-values reported are Bonferroni corrected and Benjamini and Hochber corrected. The full microarray dataset is available at GEO under accession number GSE57352. Genes included in Table 1 comprise a subset upregulated by AGN193109/downregulated by TTNPB based on their regional expression in the posterior.

Embryo microinjection

Xenopus eggs were fertilized *in vitro* and embryos staged as described (Janesick et al., 2012). Embryos were injected bilaterally or unilaterally at the 2- or 4-cell stage with gene-specific morpholinos (MOs) (supplementary material Table S1) and/or mRNA together with 100 pg/embryo β -galactosidase (β -gal) mRNA. For all MO experiments, control embryos were injected with 10 ng standard control MO (GeneTools). Embryos were maintained in 0.1 \times MBS until appropriate stages. Embryos processed for WISH were fixed in MEMFA, stained with magenta-GAL (Biosynth), and then stored in 100% ethanol (Janesick et al., 2012).

pCDG1-DN-*xRary2* was constructed by cloning amino acids 1-393 (lacking the AF-2 domain) into the *NcoI*-*BamHI* site of pCDG1 (Blumberg et al., 1998). pCDG1-VP16-*xRary2* was constructed by cloning the VP16 activation domain upstream of *xRary2* into pCDG1. pCDG1-*xRara2*, pCMX-GAL4-*Rara* and GAL4-*Rary* were from Blumberg et al. (Blumberg et al., 1996). *X. laevis* *Rar β 1* and *Rar β 2* sequences were found by aligning to the *X. tropicalis* sequences. pCDG1-*xRar β 2* and pCMX-GAL4-*xRar β* cloning primers are listed in supplementary material Table S2. pCDG1-*xCyp26a1* and pCDG1-*c-smrt* were constructed by PCR amplification of *xCyp26a1* coding regions (Holleman et al., 1998) or *Xl c-smrt* (37b-, 41+) (Chen et al., 1996; Malartre et al., 2004) and cloning into pCDG1.

xRara1^{EGCKG→GSKCV}, *xRara2*^{EGCKG→GSKCV}, *xRar β 2*^{EGCKG→GSKCV}, *xRary1*^{EGCKG→GSKCV} and *xRary2*^{EGCKG→GSKCV} were designed according to Klein et al. (1996), constructed by two-fragment PCR, and cloned into pCDG1 (primer sequences are provided in supplementary material Table S3). Four copies of RXRE^{1/2}-GRE^{1/2} (GGAAGGGTTCACCGAA-AGAACACTCGC) were cloned upstream of the TK-luciferase reporter. All pCDG1 plasmids were sequence verified, linearized with *NotI*, and mRNA transcribed using mMessage mMachine T7 (Ambion). pCS2-*mCherry* was linearized with *NotI* and transcribed from the SP6 promoter.

Embryo treatments and reporter assays

Microinjected embryos were treated at stage 8 with the following chemicals (in 0.1 \times MBS): TTNPB (RAR agonist), NRX204647 (RAR γ -selective agonist), NRX205099 (RAR γ -selective inverse agonist) or 0.1% ethanol vehicle. Twenty-five embryos were treated in each 60-mm Petri dish containing 10 ml chemical. Treated embryos were fixed in MEMFA and processed for WISH, or separated into five-embryo aliquots at stage 10.5 for luciferase assays, or separated into five-embryo aliquots at neurula or tailbud stage for QPCR as described (Janesick et al., 2012). Each group of five embryos was considered one biological replicate ($n=1$).

WISH

Embryos were microinjected or treated with chemicals after the completion of gastrulation (stage 12.5). WISH was performed as previously described (Janesick et al., 2012). *Rary1*, *Rary2*, *Rara* (Blumberg et al., 1992), *Hoxc10*, *Ripply2*, *Thyl2*, *Mgn1* (Klein et al., 2002), *Hoxd10* (Lombardo and Slack, 2001), *Tbx6* (Uchiyama et al., 2001), *Raldh2* (Glinka et al., 1996) and *Myod* (Hopwood et al., 1989) probes were prepared by PCR amplification of coding regions from cDNA with T7 promoter at the 3' end and *in vitro* transcribed. *Hoxc13* sequence was derived from EST clone XL042b19. Relevant primers

are listed in supplementary material Table S4. *Krox20* (Bradley et al., 1993) and *En2* (Bolce et al., 1992) probes were made using T7 and T3 polymerase from *EcoRI* and *XbaI* linearized plasmids, respectively. Probes were transcribed with MEGAscript T7 (Ambion) in the presence of digoxigenin-11-UTP (Roche). Double WISH was conducted as described (Janesick et al., 2012). DNP-*Rary2* was transcribed in the presence of dinitrophenol-11-UTP (PerkinElmer). *Hoxc10* expression was quantitated using MATLAB (MathWorks) (supplementary material Fig. S8). The number of purple pixels was calculated by thresholding individual RGB channels (R&B>170, G>120) and dividing by the total number of pixels occupied by the embryo.

Transfection

1 μ g CMX-*Rar*^{EGCKG→GSKCV} effector plasmid was co-transfected with 5 μ g tk-(RXRE^{1/2}-GRE^{1/2}) \times 4 luciferase reporter and 5 μ g pCMX- β -galactosidase transfection control plasmids as previously described (Chamorro-Garcia et al., 2012). For activation assays, NRX204647 was tested from 10⁻¹¹ M to 10⁻⁵ M. For antagonism assays, NRX205099 was tested from 10⁻¹⁰ M to 10⁻⁵ M against 10⁻⁸ M 9-cis RA. All transfections were performed in triplicate and reproduced in multiple experiments. Data are reported as normalized luciferase \pm s.e.m. or percentage reduction \pm s.e.m. using standard propagation of error (Bevington and Robinson, 2003).

Quantitative real-time reverse transcription PCR (QPCR)

Total RNA from five-embryo pools was DNase treated, LiCl precipitated, and reverse transcribed into cDNA (Janesick et al., 2012). First-strand cDNA was quantitated in a Light Cycler 480 System (Roche) using primer sets listed in supplementary material Table S5 and SYBR Green. Each primer set amplified a single band as determined by gel electrophoresis and melting curve analysis. QPCR data for supplementary material Figs S2 and S7 were analyzed by Δ Ct relative to *Histone H4*, correcting for amplification efficiency between RARs (Pfaffl, 2001). QPCR data for supplementary material Figs S11 and S12 were analyzed by $\Delta\Delta$ Ct relative to *Histone H4*, normalizing to control embryos. Error bars represent biological replicates calculated using standard propagation of error.

Acknowledgements

We thank Connie Chung for technical help during the early stages of this study and Dr Dennis Bittner for editorial assistance.

Competing interests

The authors declare no competing financial interests.

Author contributions

T.T.L.N. performed WISH. K.A., K.I., S.K. and J.K. executed the Perccellome microarray experiment. R.A.S.C. provided 4647 and 5099 chemicals with advice on use. A.J. and B.B. designed, supervised and performed experiments, and wrote, edited and submitted the manuscript.

Funding

Supported by grants from the National Science Foundation (NSF) [IOS-0719576, IOS-1147236 to B.B.]. A.J. was a predoctoral trainee of NSF IGERT DGE 0549479. K.I., S.K. and J.K. were funded by Health Sciences Research Grant H15-kagaku-002 from the Ministry of Health, Labour and Welfare, Japan.

Supplementary material

Supplementary material available online at <http://dev.biologists.org/lookup/suppl/doi:10.1242/dev.103705/-DC1>

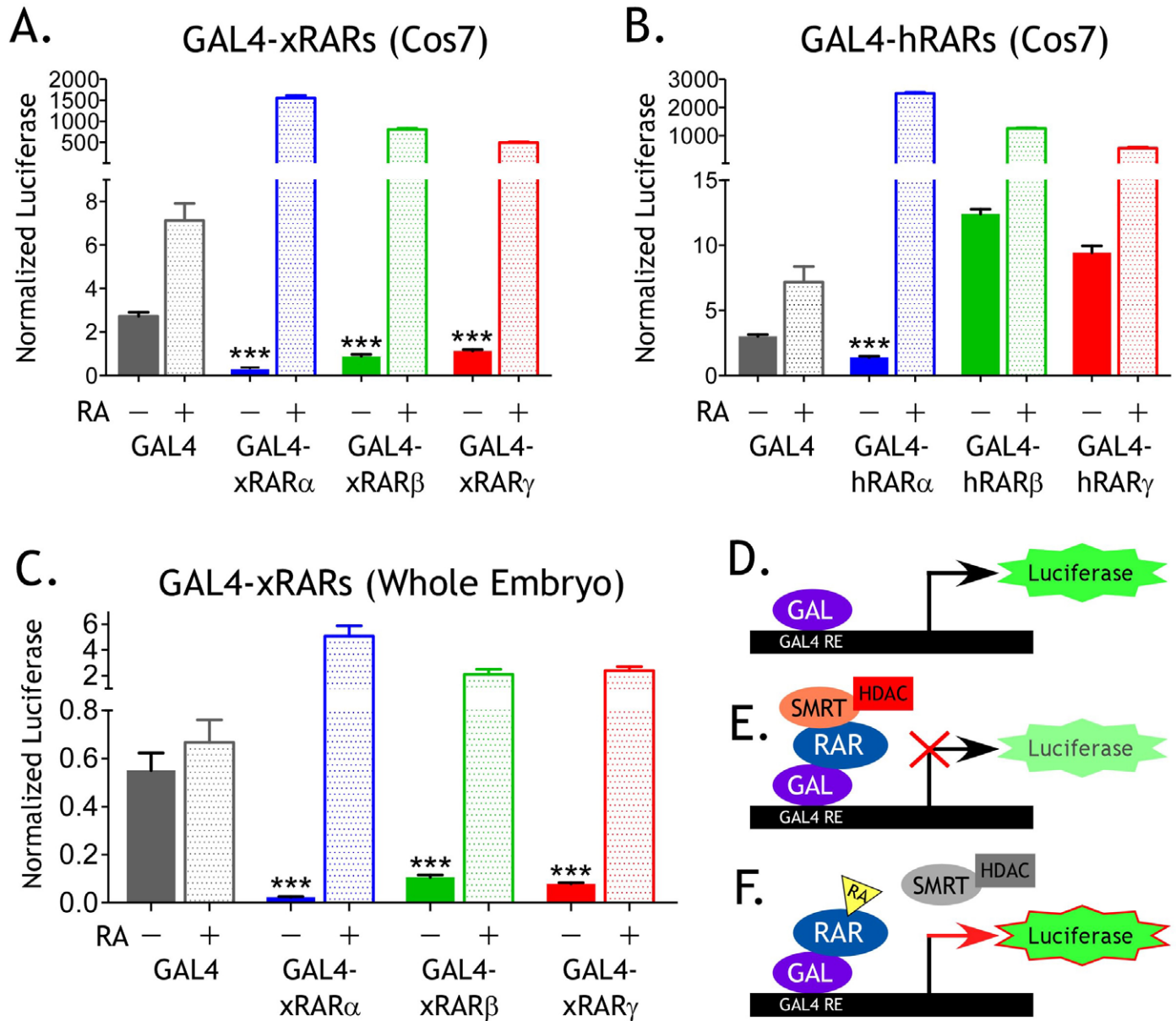
References

- Abu-Abed, S., Dollé, P., Metzger, D., Beckett, B., Chambon, P. and Petkovich, M. (2001). The retinoic acid-metabolizing enzyme, CYP26A1, is essential for normal hindbrain patterning, vertebral identity, and development of posterior structures. *Genes Dev.* **15**, 226-240.
- Arima, K., Shiotsugu, J., Niu, R., Khandpur, R., Martinez, M., Shin, Y., Koide, T., Cho, K. W. Y., Kitayama, A., Ueno, N. et al. (2005). Global analysis of RAR-responsive genes in the *Xenopus* neurula using cDNA microarrays. *Dev. Dyn.* **232**, 414-431.
- Beck, C. W. and Slack, J. M. W. (1998). Analysis of the developing *Xenopus* tail bud reveals separate phases of gene expression during determination and outgrowth. *Mech. Dev.* **72**, 41-52.
- Bevington, P. R. and Robinson, D. K. (2003). *Data Reduction and Error Analysis for the Physical Sciences*. New York: McGraw-Hill Education.

- Blewitt, R.** (2009). Enhancer of split-related-2 mRNA shows cyclic expression during somitogenesis in *Xenopus laevis*. *Biosci. Horizons* **2**, 22-31.
- Blumberg, B., Mangelsdorf, D. J., Dyck, J. A., Bittner, D. A., Evans, R. M. and De Robertis, E. M.** (1992). Multiple retinoid-responsive receptors in a single cell: families of retinoid "X" receptors and retinoic acid receptors in the *Xenopus* egg. *Proc. Natl. Acad. Sci. U.S.A.* **89**, 2321-2325.
- Blumberg, B., Bolado, J., Jr, Derguini, F., Craig, A. G., Moreno, T. A., Chakravarti, D., Heyman, R. A., Buck, J. and Evans, R. M.** (1996). Novel retinoic acid receptor ligands in *Xenopus* embryos. *Proc. Natl. Acad. Sci. U.S.A.* **93**, 4873-4878.
- Blumberg, B., Bolado, J., Jr, Moreno, T. A., Kintner, C., Evans, R. M. and Papalopulu, N.** (1997). An essential role for retinoid signaling in anteroposterior neural patterning. *Development* **124**, 373-379.
- Blumberg, B., Kang, H., Bolado, J., Chen, H., Craig, A. G., Moreno, T. A., Umesono, K., Perlmann, T., De Robertis, E. M. and Evans, R. M.** (1998). BXR, an embryonic orphan nuclear receptor activated by a novel class of endogenous benzoate metabolites. *Genes Dev.* **12**, 1269-1277.
- Bolce, M. E., Hemmati-Brivanlou, A., Kushner, P. D. and Harland, R. M.** (1992). Ventral ectoderm of *Xenopus* forms neural tissue, including hindbrain, in response to activin. *Development* **115**, 681-688.
- Bradley, L. C., Snape, A., Bhatt, S. and Wilkinson, D. G.** (1993). The structure and expression of the *Xenopus* Krox-20 gene: conserved and divergent patterns of expression in rhombomeres and neural crest. *Mech. Dev.* **40**, 73-84.
- Buchberger, A., Bonneick, S. and Arnold, H.-H.** (2000). Expression of the novel basic-helix-loop-helix transcription factor cMespo in presomitic mesoderm of chicken embryos. *Mech. Dev.* **97**, 223-226.
- Cambay, N. and Wilson, V.** (2002). Axial progenitors with extensive potency are localised to the mouse chordeuronal hinge. *Development* **129**, 4855-4866.
- Cambay, N. and Wilson, V.** (2007). Two distinct sources for a population of maturing axial progenitors. *Development* **134**, 2829-2840.
- Chakravarti, D., LaMorte, V. J., Nelson, M. C., Nakajima, T., Schulman, I. G., Juguilon, H., Montminy, M. and Evans, R. M.** (1996). Role of CBP/P300 in nuclear receptor signalling. *Nature* **383**, 99-103.
- Chamorro-García, R., Kirchner, S., Li, X., Janesick, A., Casey, S. C., Chow, C. and Blumberg, B.** (2012). Bisphenol A diglycidyl ether induces adipogenic differentiation of multipotent stromal stem cells through a peroxisome proliferator-activated receptor gamma-independent mechanism. *Environ. Health Perspect.* **120**, 984-989.
- Chen, J. D. and Evans, R. M.** (1995). A transcriptional co-repressor that interacts with nuclear hormone receptors. *Nature* **377**, 454-457.
- Chen, J. D., Umesono, K. and Evans, R. M.** (1996). SMRT isoforms mediate repression and anti-repression of nuclear receptor heterodimers. *Proc. Natl. Acad. Sci. U.S.A.* **93**, 7567-7571.
- Dahmann, C., Oates, A. C. and Brand, M.** (2011). Boundary formation and maintenance in tissue development. *Nat. Rev. Genet.* **12**, 43-55.
- Davis, R. L. and Kirschner, M. W.** (2000). The fate of cells in the tailbud of *Xenopus laevis*. *Development* **127**, 255-267.
- de Roos, K., Sonneveld, E., Compaan, B., ten Berge, D., Durston, A. J. and van der Saag, P. T.** (1999). Expression of retinoic acid 4-hydroxylase (CYP26) during mouse and *Xenopus laevis* embryogenesis. *Mech. Dev.* **82**, 205-211.
- Dequérant, M.-L. and Pourquié, O.** (2008). Segmental patterning of the vertebrate embryonic axis. *Nat. Rev. Genet.* **9**, 370-382.
- Dubrulle, J., McGrew, M. J. and Pourquié, O.** (2001). FGF signaling controls somite boundary position and regulates segmentation clock control of spatiotemporal Hox gene activation. *Cell* **106**, 219-232.
- Escriba, H., Bertrand, S., Germain, P., Robinson-Rechavi, M., Umbhauer, M., Carry, J., Duffraisse, M., Holland, L., Gronemeyer, H. and Laudet, V.** (2006). Neofunctionalization in vertebrates: the example of retinoic acid receptors. *PLoS Genet.* **2**, e102.
- Fior, R., Maxwell, A. A., Ma, T. P., Vezaro, A., Moens, C. B., Amacher, S. L., Lewis, J. and Saude, L.** (2012). The differentiation and movement of presomitic mesoderm progenitor cells are controlled by Mesogenin 1. *Development* **139**, 4656-4665.
- Fujii, H., Sato, T., Kaneko, S., Gotoh, O., Fujii-Kuriyama, Y., Osawa, K., Kato, S. and Hamada, H.** (1997). Metabolic inactivation of retinoic acid by a novel P450 differentially expressed in developing mouse embryos. *EMBO J.* **16**, 4163-4173.
- Gabellini, D., Colaluca, I. N., Vodermaier, H. C., Biamonti, G., Giacca, M., Falaschi, A., Riva, S. and Peverali, F. A.** (2003). Early mitotic degradation of the homeoprotein HOXC10 is potentially linked to cell cycle progression. *EMBO J.* **22**, 3715-3724.
- Glinka, A., Delius, H., Blumenstock, C. and Niehrs, C.** (1996). Combinatorial signalling by Xwnt-11 and Xnr3 in the organizer epithelium. *Mech. Dev.* **60**, 221-231.
- Gomez, C. and Pourquié, O.** (2009). Developmental control of segment numbers in vertebrates. *J. Exp. Zool. B Mol. Dev. Evol.* **312B**, 533-544.
- Hitachi, K., Kondow, A., Danno, H., Inui, M., Uchiyama, H. and Asashima, M.** (2008). Tbx6, Thylacine1, and E47 synergistically activate bowline expression in *Xenopus* somitogenesis. *Dev. Biol.* **313**, 816-828.
- Holleman, T., Chen, Y., Grunz, H. and Pieler, T.** (1998). Regionalized metabolic activity establishes boundaries of retinoic acid signalling. *EMBO J.* **17**, 7361-7372.
- Hopwood, N. D., Pluck, A. and Gurdon, J. B.** (1989). MyoD expression in the forming somites is an early response to mesoderm induction in *Xenopus* embryos. *EMBO J.* **8**, 3409-3417.
- Iimura, T., Denans, N. and Pourquié, O.** (2009). Establishment of Hox vertebral identities in the embryonic spine precursors. *Curr. Top. Dev. Biol.* **88**, 201-234.
- Janesick, A., Shiotsugu, J., Taketani, M. and Blumberg, B.** (2012). RIPPLY3 is a retinoic acid-inducible repressor required for setting the borders of the pre-placodal ectoderm. *Development* **139**, 1213-1224.
- Janesick, A., Abbey, R., Chung, C., Liu, S., Taketani, M. and Blumberg, B.** (2013). ERF and ETV3L are retinoic acid-inducible repressors required for primary neurogenesis. *Development* **140**, 3095-3106.
- Kanno, J., Aisaki, K.-i., Igarashi, K., Nakatsu, N., Ono, A., Kodama, Y. and Nagao, T.** (2006). "Per cell" normalization method for mRNA measurement by quantitative PCR and microarrays. *BMC Genomics* **7**, 64.
- Kayala, M. A. and Baldi, P.** (2012). Cyber-T web server: differential analysis of high-throughput data. *Nucleic Acids Res.* **40**, W553-W559.
- Klein, E. S., Pino, M. E., Johnson, A. T., Davies, P. J. A., Nagpal, S., Thacher, S. M., Krasinski, G. and Chandraratna, R. A. S.** (1996). Identification and functional separation of retinoic acid receptor neutral antagonists and inverse agonists. *J. Biol. Chem.* **271**, 22692-22696.
- Klein, S. L., Strausberg, R. L., Wagner, L., Pontius, J., Clifton, S. W. and Richardson, P.** (2002). Genetic and genomic tools for *Xenopus* research: the NIH *Xenopus* initiative. *Dev. Dyn.* **225**, 384-391.
- Koide, T., Downes, M., Chandraratna, R. A. S., Blumberg, B. and Umesono, K.** (2001). Active repression of RAR signaling is required for head formation. *Genes Dev.* **15**, 2111-2121.
- Lamka, M. L., Boulet, A. M. and Sakonju, S.** (1992). Ectopic expression of UBX and ABD-B proteins during *Drosophila* embryogenesis: competition, not a functional hierarchy, explains phenotypic suppression. *Development* **116**, 841-854.
- Leroy, P., Nakshatri, H. and Chambon, P.** (1991). Mouse retinoic acid receptor alpha 2 isoform is transcribed from a promoter that contains a retinoic acid response element. *Proc. Natl. Acad. Sci. U.S.A.* **88**, 10138-10142.
- Lombardo, A. and Slack, J. M.** (2001). Abdominal B-type Hox gene expression in *Xenopus laevis*. *Mech. Dev.* **106**, 191-195.
- Malartre, M., Short, S. and Sharpe, C.** (2004). Alternative splicing generates multiple SMRT transcripts encoding conserved repressor domains linked to variable transcription factor interaction domains. *Nucleic Acids Res.* **32**, 4676-4686.
- McGrew, M. J., Sherman, A., Lillico, S. G., Ellard, F. M., Radcliffe, P. A., Gilhooley, H. J., Mitrophanous, K. A., Cambay, N., Wilson, V. and Sang, H.** (2008). Localised axial progenitor cell populations in the avian tail bud are not committed to a posterior Hox identity. *Development* **135**, 2289-2299.
- Mollard, R., Viville, S., Ward, S. J., Décimo, D., Chambon, P. and Dollé, P.** (2000). Tissue-specific expression of retinoic acid receptor isoform transcripts in the mouse embryo. *Mech. Dev.* **94**, 223-232.
- Moreno, T. A. and Kintner, C.** (2004). Regulation of segmental patterning by retinoic acid signaling during *Xenopus* somitogenesis. *Dev. Cell* **6**, 205-218.
- Nakaya, Y., Kuroda, S., Katagiri, Y. T., Kaibuchi, K. and Takahashi, Y.** (2004). Mesenchymal-epithelial transition during somitic segmentation is regulated by differential roles of Cdc42 and Rac1. *Dev. Cell* **7**, 425-438.
- Nowotschin, S., Ferrer-Vaquer, A., Concepcion, D., Papaioannou, V. E. and Hadjantonakis, A.-K.** (2012). Interaction of Wnt3a, Msn1 and Tbx6 in neural versus paraxial mesoderm lineage commitment and paraxial mesoderm differentiation in the mouse embryo. *Dev. Biol.* **367**, 1-14.
- Olivera-Martinez, I., Harada, H., Halley, P. A. and Storey, K. G.** (2012). Loss of FGF-dependent mesoderm identity and rise of endogenous retinoid signalling determine cessation of body axis elongation. *PLoS Biol.* **10**, e1001415.
- Pfaffl, M. W.** (2001). A new mathematical model for relative quantification in real-time RT-PCR. *Nucleic Acids Res.* **29**, e45.
- Pfeffer, P. L. and De Robertis, E. M.** (1994). Regional specificity of RAR gamma isoforms in *Xenopus* development. *Mech. Dev.* **45**, 147-153.
- Pourquié, O. and Tam, P. P. L.** (2001). A nomenclature for prospective somites and phases of cyclic gene expression in the presomitic mesoderm. *Dev. Cell* **1**, 619-620.
- Rhinn, M. and Dolle, P.** (2012). Retinoic acid signalling during development. *Development* **139**, 843-858.
- Sakai, Y., Meno, C., Fujii, H., Nishino, J., Shiratori, H., Saijoh, Y., Rossant, J. and Hamada, H.** (2001). The retinoic acid-inactivating enzyme CYP26 is essential for establishing an uneven distribution of retinoic acid along the antero-posterior axis within the mouse embryo. *Genes Dev.* **15**, 213-225.
- Shimono, K., Tung, W.-e., Macolino, C., Chi, A. H.-T., Didizian, J. H., Mundy, C., Chandraratna, R. A., Mishina, Y., Enomoto-Iwamoto, M., Pacifici, M. et al.** (2011). Potent inhibition of heterotopic ossification by nuclear retinoic acid receptor-gamma agonists. *Nat. Med.* **17**, 454-460.

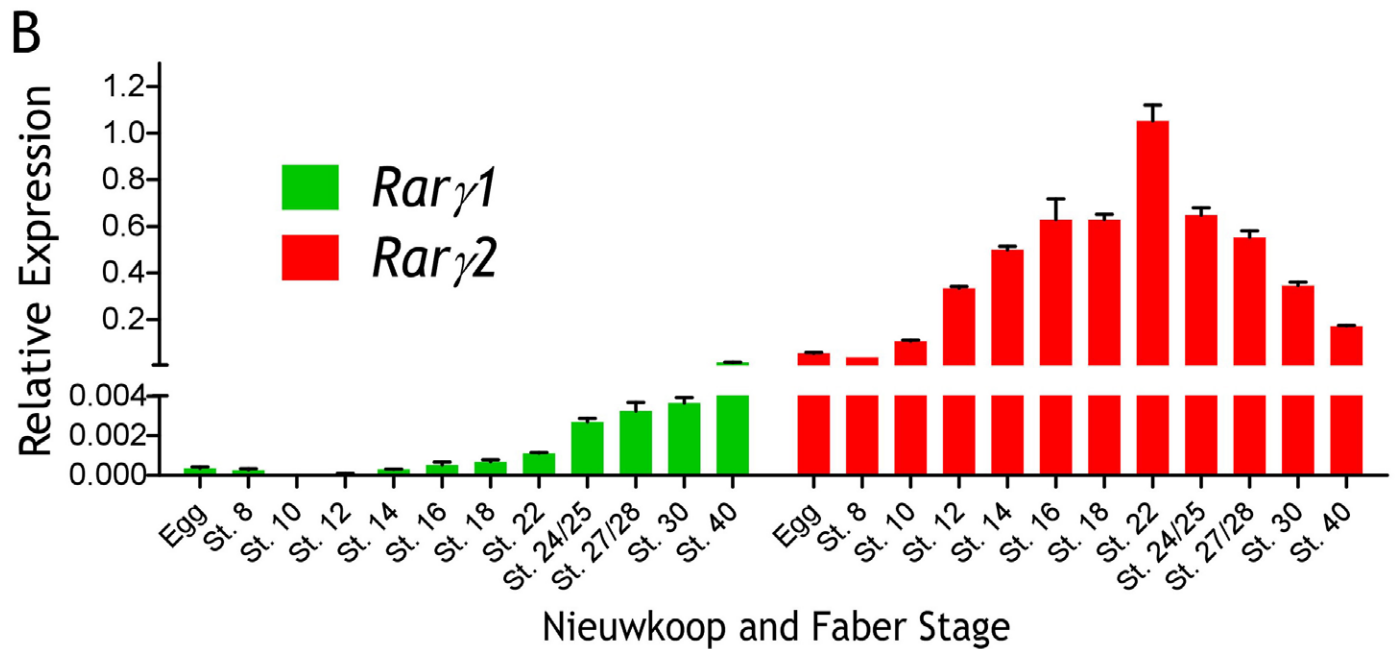
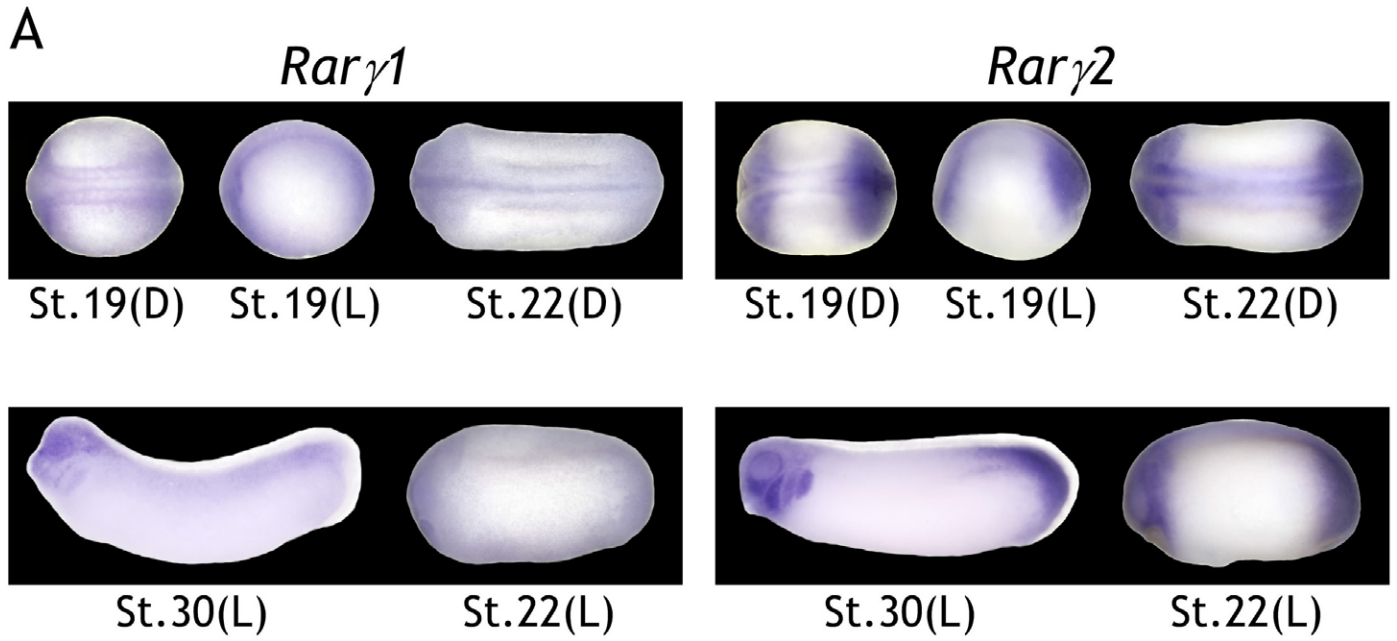
- Shum, A. S. W., Poon, L. L. M., Tang, W. W. T., Koide, T., Chan, B. W. H., Leung, Y.-C. G., Shiroishi, T. and Copp, A. J.** (1999). Retinoic acid induces down-regulation of Wnt-3a, apoptosis and diversion of tail bud cells to a neural fate in the mouse embryo. *Mech. Dev.* **84**, 17-30.
- Sive, H. L., Draper, B. W., Harland, R. M. and Weintraub, H.** (1990). Identification of a retinoic acid-sensitive period during primary axis formation in *Xenopus laevis*. *Genes Dev.* **4**, 932-942.
- Sucov, H. M., Murakami, K. K. and Evans, R. M.** (1990). Characterization of an autoregulated response element in the mouse retinoic acid receptor type beta gene. *Proc. Natl. Acad. Sci. U.S.A.* **87**, 5392-5396.
- Takemoto, T., Uchikawa, M., Yoshida, M., Bell, D. M., Lovell-Badge, R., Papaioannou, V. E. and Kondoh, H.** (2011). Tbx6-dependent Sox2 regulation determines neural or mesodermal fate in axial stem cells. *Nature* **470**, 394-398.
- Tam, P. P. L., Goldman, D., Camus, A. and Schoenwolf, G. C.** (2000). 1 Early events of somitogenesis in higher vertebrates: allocation of precursor cells during gastrulation and the organization of a meristic pattern in the paraxial mesoderm. *Curr. Top. Dev. Biol.* **47**, 1-32.
- Thacher, S. M., Vasudevan, J. and Chandraratna, R. A. S.** (2000). Therapeutic applications for ligands of retinoid receptors. *Curr. Pharm. Des.* **6**, 25-58.
- Tsang, K. Y., Sinha, S., Liu, X., Bhat, S. and Chandraratna, R., A.** (2003). Disubstituted Chalcone Oximes Having Rar(Gamma)-Retinoid Receptor Antagonist Activity. European Patent Office.
- Uchiyama, H., Kobayashi, T., Yamashita, A., Ohno, S. and Yabe, S.** (2001). Cloning and characterization of the T-box gene Tbx6 in *Xenopus laevis*. *Dev. Growth Differ.* **43**, 657-669.
- von Dassow, G., Schmidt, J. E. and Kimelman, D.** (1993). Induction of the *Xenopus* organizer: expression and regulation of Xnot, a novel FGF and activin-regulated homeo box gene. *Genes Dev.* **7**, 355-366.
- Wellik, D. M.** (2007). Hox patterning of the vertebrate axial skeleton. *Dev. Dyn.* **236**, 2454-2463.
- Weston, A. D., Blumberg, B. and Underhill, T. M.** (2003). Active repression by unliganded retinoid receptors in development: less is sometimes more. *J. Cell Biol.* **161**, 223-228.
- Wong, C. W. and Privalsky, M. L.** (1998). Transcriptional silencing is defined by isoform- and heterodimer-specific interactions between nuclear hormone receptors and corepressors. *Mol. Cell Biol.* **18**, 5724-5733.
- Yabe, T. and Takada, S.** (2012). Mesogenin causes embryonic mesoderm progenitors to differentiate during development of zebrafish tail somites. *Dev. Biol.* **370**, 213-222.
- Yoon, J. K. and Wold, B.** (2000). The bHLH regulator pMesogenin1 is required for maturation and segmentation of paraxial mesoderm. *Genes Dev.* **14**, 3204-3214.
- Yoon, J. K., Moon, R. T. and Wold, B.** (2000). The bHLH class protein pMesogenin1 can specify paraxial mesoderm phenotypes. *Dev. Biol.* **222**, 376-391.
- Young, T., Rowland, J. E., van de Ven, C., Bialecka, M., Novoa, A., Carapuco, M., van Nes, J., de Graaff, W., Duluc, I., Freund, J.-N. et al.** (2009). Cdx and Hox genes differentially regulate posterior axial growth in mammalian embryos. *Dev. Cell* **17**, 516-526.

Supplemental Figure S1



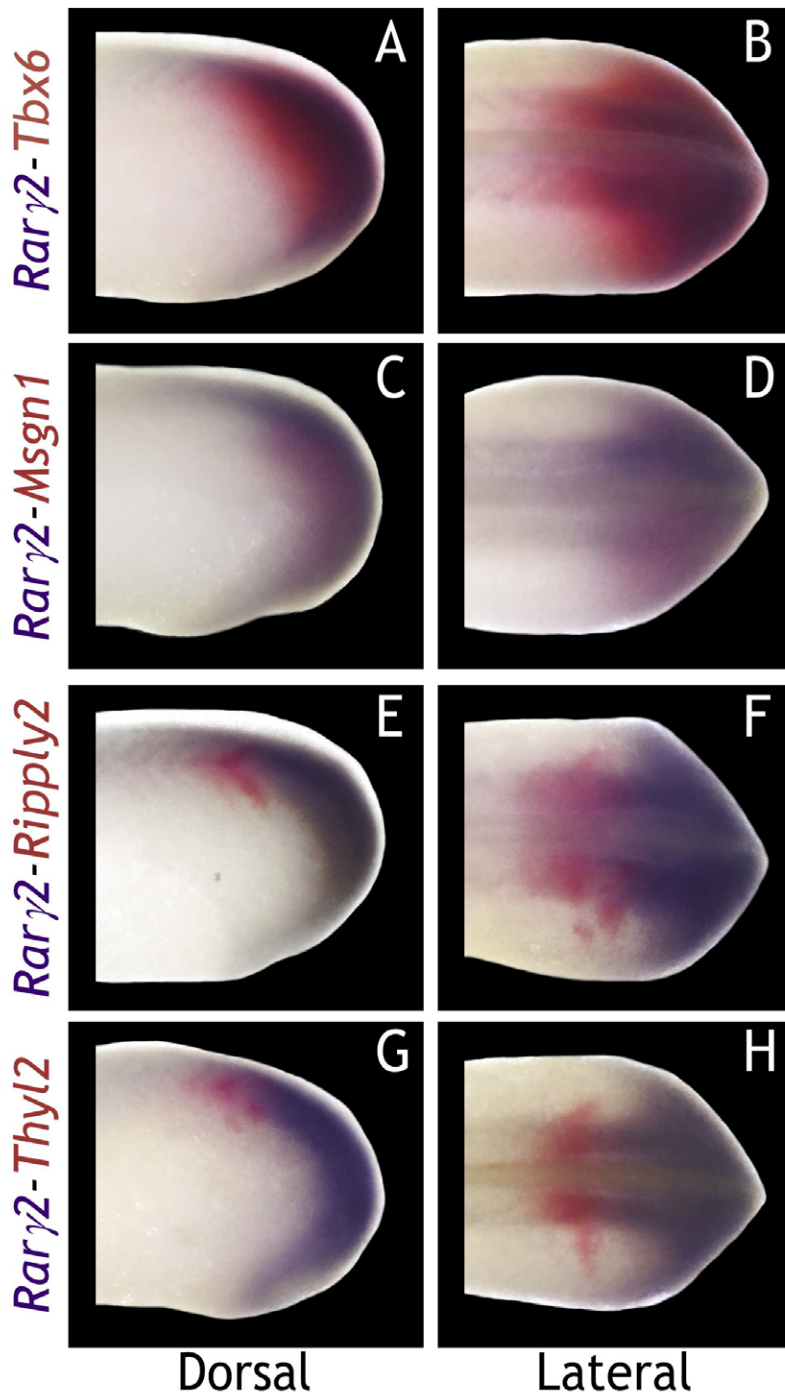
Supplemental Figure S1. *Xenopus laevis* RARs repress basal transcriptional activity. (A, B) Cos7 cells were transfected with 5:5:1 DNA ratio of reporter : β -gal : Gal4-RAR (or Gal4 alone), and treated with 10 μ M 9-cis RA or vehicle (0.1% DMSO). The y-axes represent relative light units measured by the luminometer normalized to β -gal activity (A, B) or embryo number (C). Basal reporter activity (A, B-gray bars, D) is repressed by xRAR α (A-blue bar, E), hRAR α (B-blue bar, E), xRAR β (A-green bar, E), and xRAR γ (A-red bar, E), but not repressed by hRAR β (B-green bar), or hRAR γ (B-red bar). (A, B, F) RA activates xRARs and hRARs. (C) Embryos were injected unilaterally at the 2- or 4-cell stage with 50 pg reporter DNA and 50 pg Gal4-xRar mRNA then treated at stage 9 with 1 μ M 9-cis RA or vehicle (0.1% EtOH). Basal reporter activity (C-gray bar, D) is repressed by xRAR α (C-blue bar, E), xRAR β (C-green bar, E), and xRAR γ (C-red bar, E). (C, F) RA relieves repression and activates xRARs. Statistical significance was determined using unpaired t-test in GraphPad Prism v5.0. Asterisks represent statistical significance compared to reporter alone (***) $P \leq 0.001$.

Supplemental Figure S2



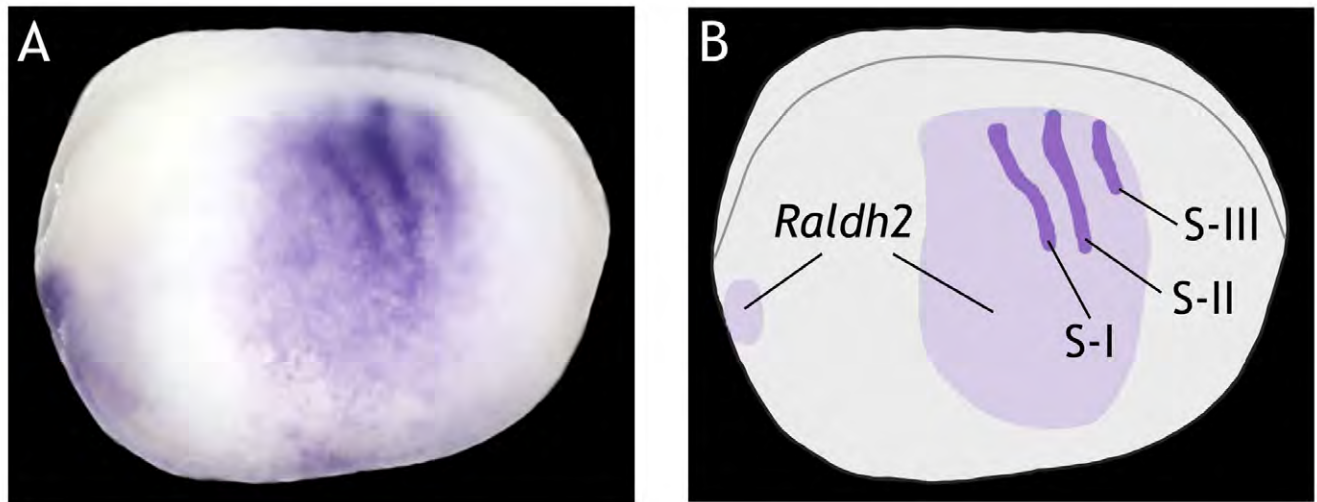
Supplemental Figure S2. Expression of *Rar γ 1* and *Rar γ 2*. (A) WISH of *Rar γ 1* and *Rar γ 2* mRNA expression at stages 19, 22, and 30. Dorsal (D) and lateral (L) views are shown with anterior to the left. (B) QPCR showing developmental expression of *Rar γ 1* and *Rar γ 2* mRNAs. The y-axis represents $2^{-\Delta Ct}$ values (adjusted for primer efficiency), normalized to reference gene, *Histone H4*.

Supplemental Figure S3



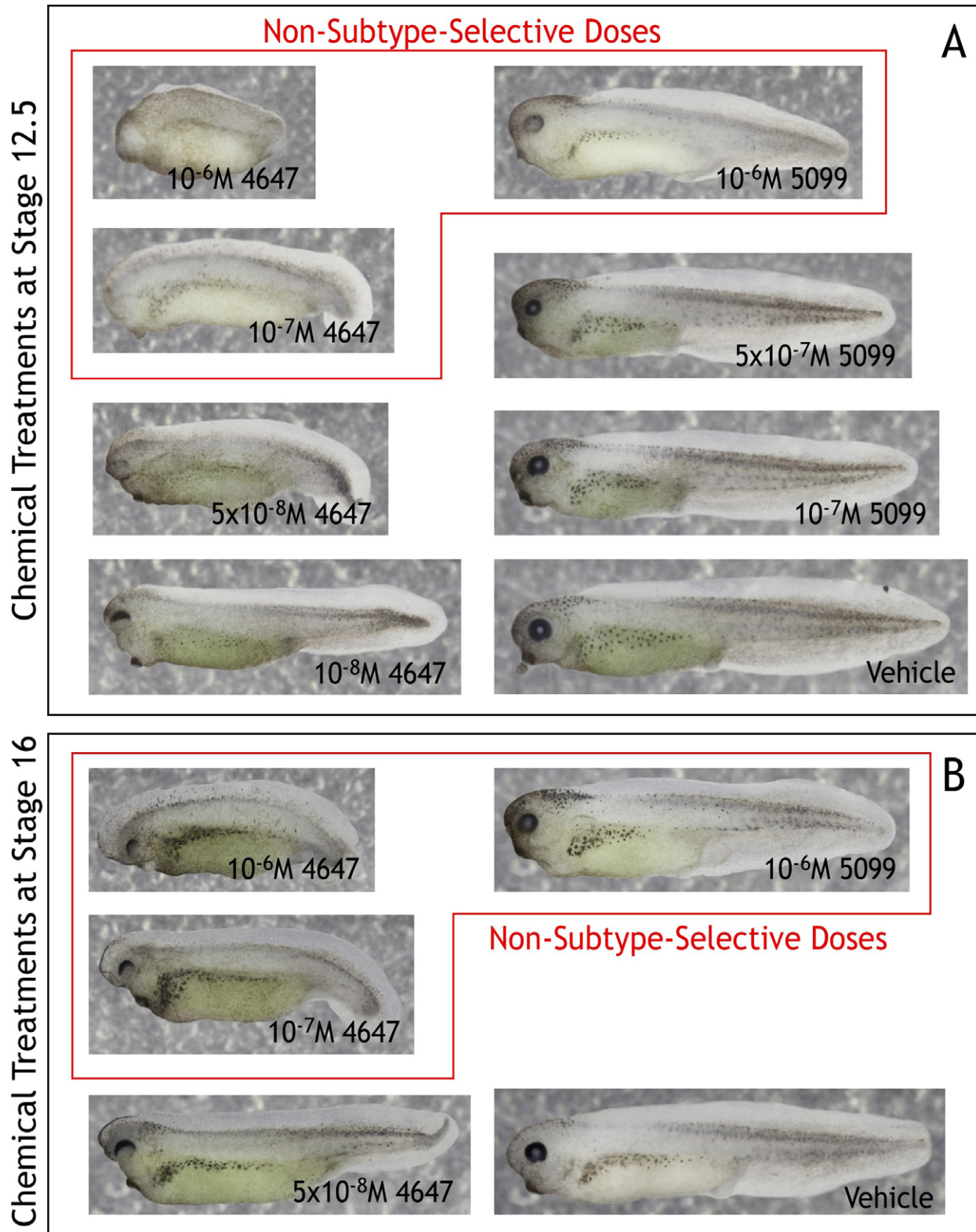
Supplemental Figure S3. Double WISH Reveals Spatial Relationship between *Rary2* and presomitic mesoderm genes at the tailbud stage. (A-H) *Rary2* is stained with BM Purple and presomitic mesoderm genes are stained with Fast Red. *Rary2* is caudal to *Tbx6* (A, B), but is synexpressed with *Msgn1* (C, D). *Rary2* overlaps with S-III domains of *Ripply2* (E, F) and *Thyl2* (G, H), but not with more anterior somitomers (S-II, S-I, S0). Dorsal and lateral views are shown with anterior to the left.

Supplemental Figure S4



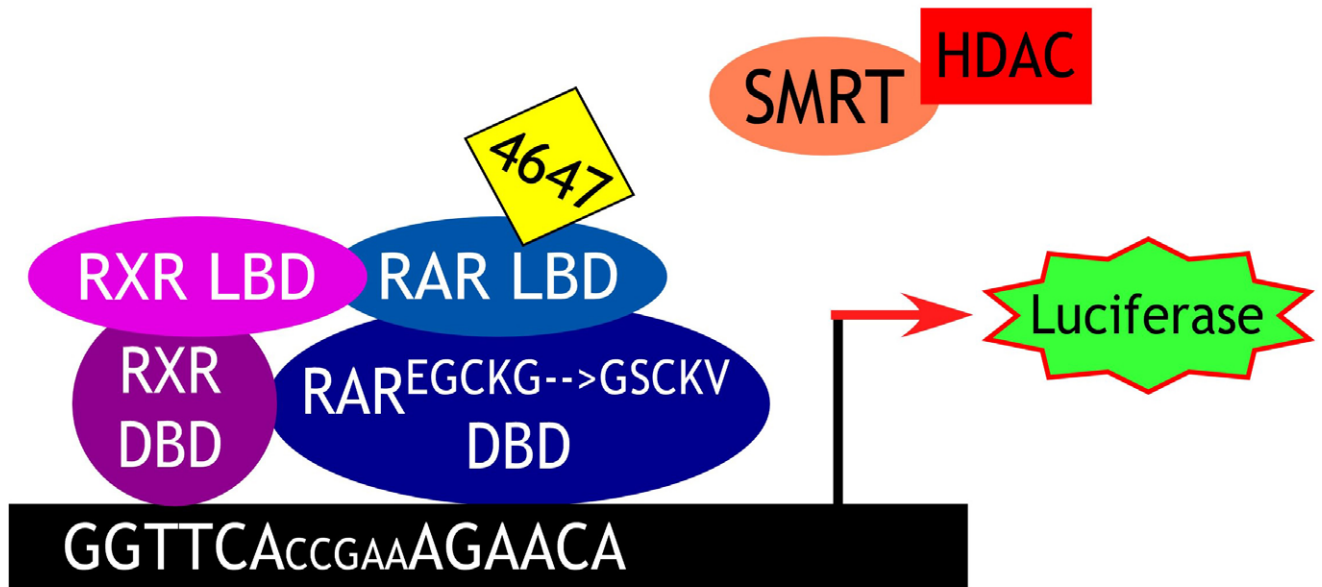
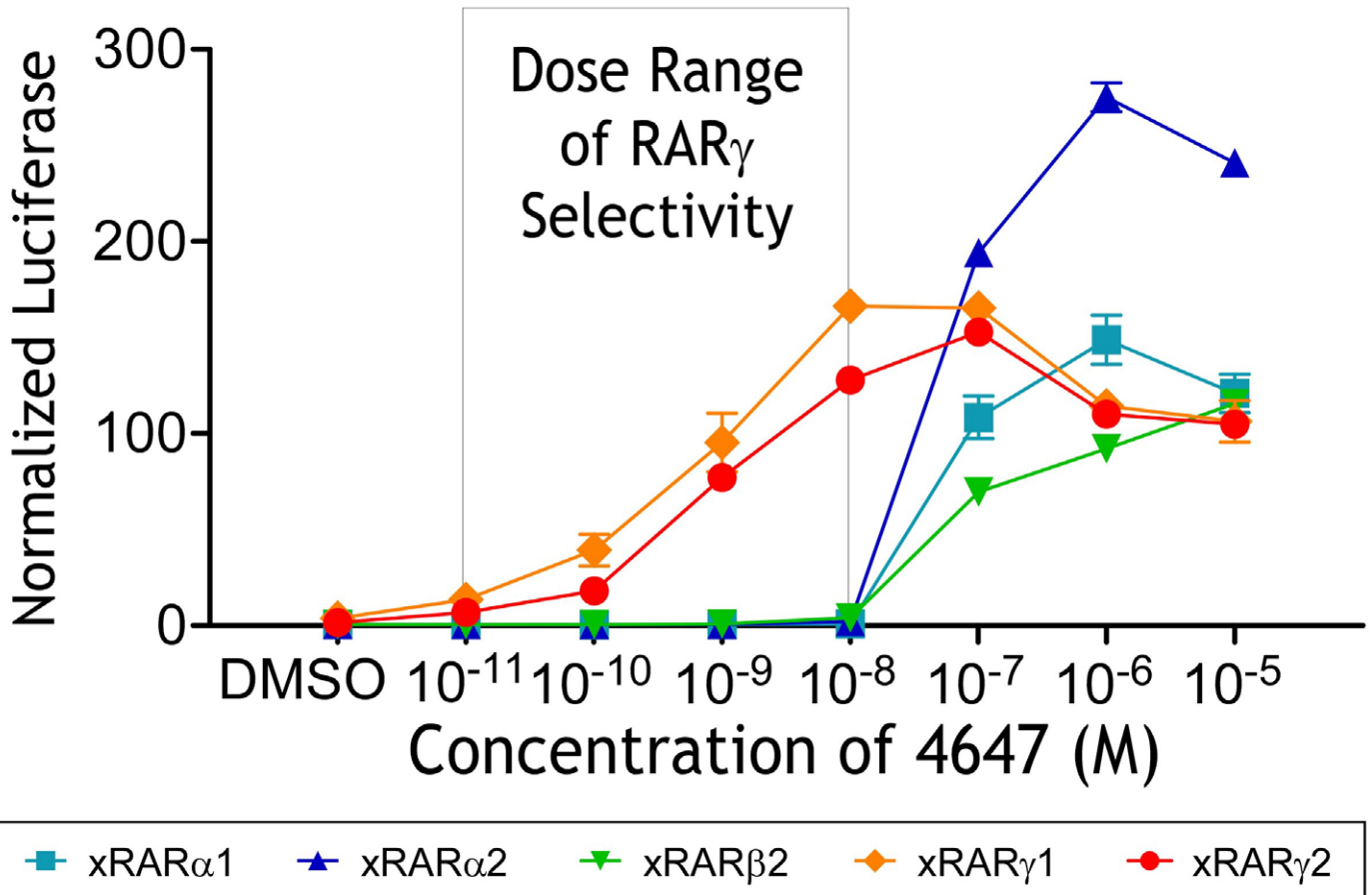
Supplemental Figure S4. Double WISH Reveals Spatial Relationship between *Raldh2* and *Thyl2*. (A) *Raldh2* overlaps all somitomere domains (S-III, S-II, S-I) of *Thyl2*. (B) Graphical representation of (A). Lateral views are shown with anterior to the left.

Supplemental Figure S5



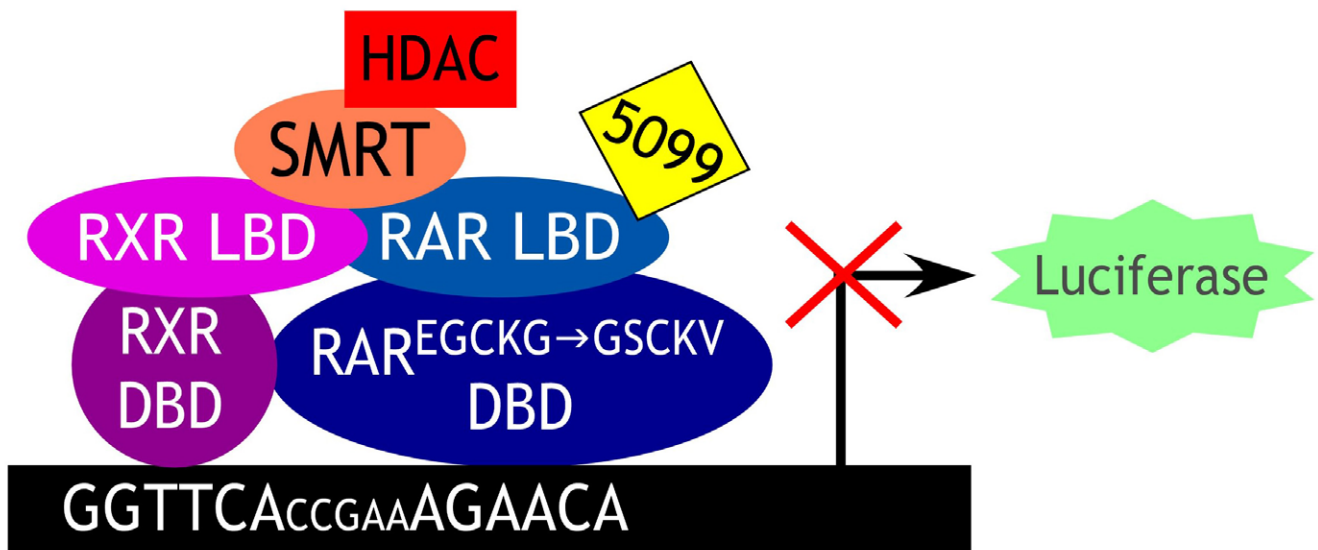
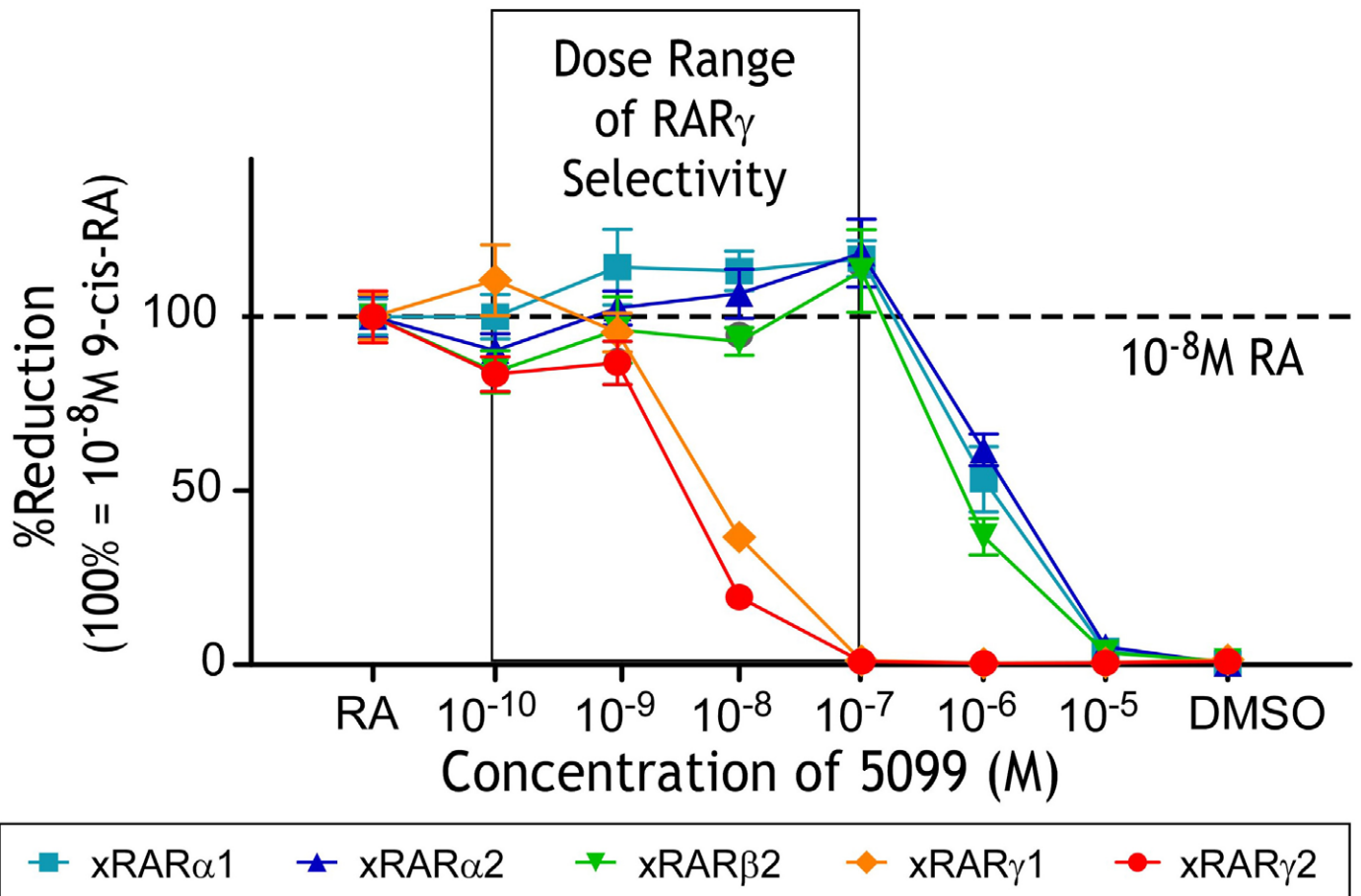
Supplemental Figure S5. Late-stage phenotypes of RAR γ -selective chemicals 4647 and 5099. (A) Embryos treated post-gastrulation (stage 12.5) with 1 μM -10 nM 4647, or 1 μM -0.1 μM 5099, or vehicle (0.1% EtOH). **(B)** Embryos treated at neurula stage 16 with 1 μM - 50 nM 4647, or 1 μM 5099, or vehicle (0.1% EtOH). Embryos are shown in lateral view at stage 40; anterior is on the left.

Supplemental Figure S6A



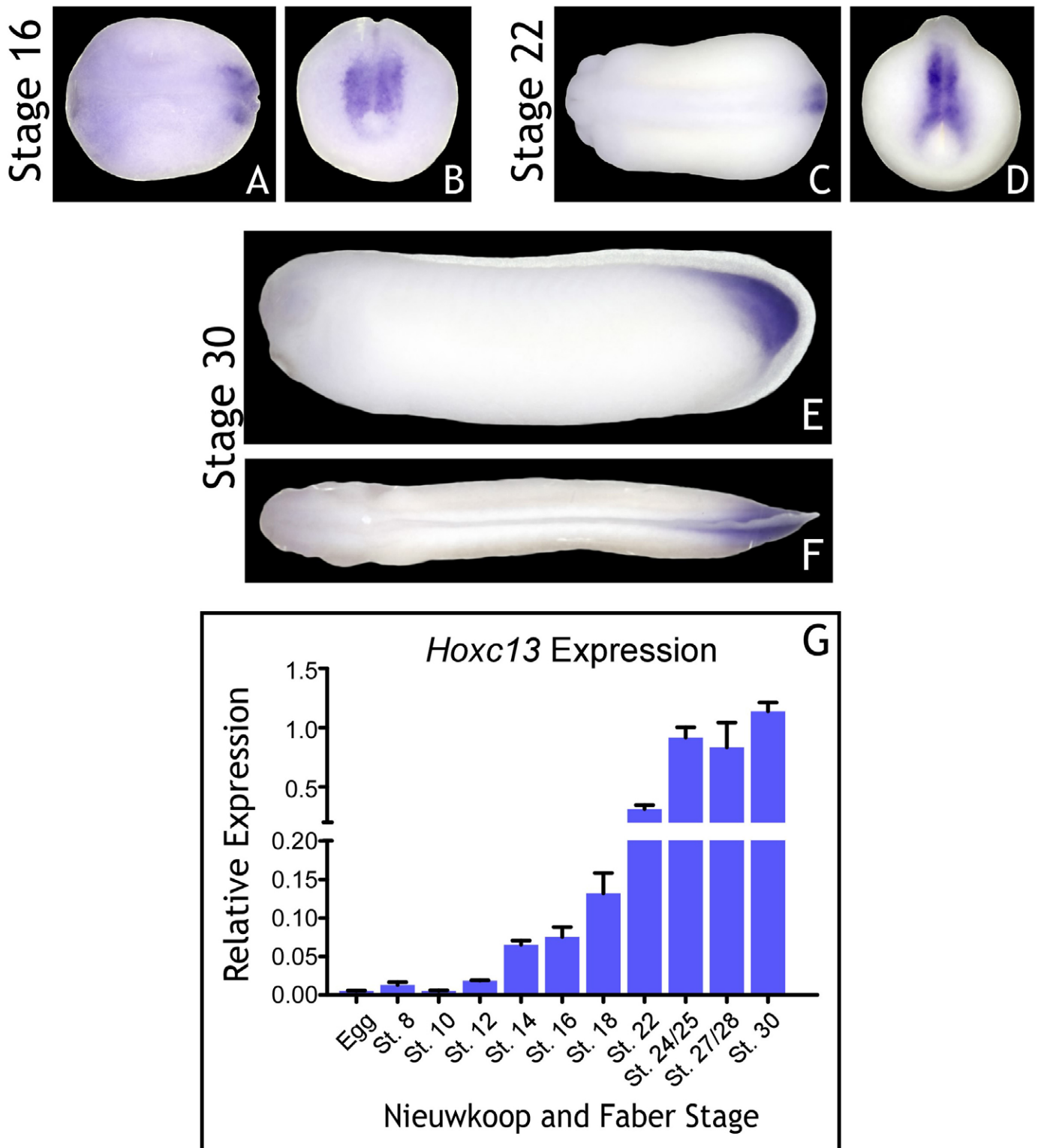
Supplemental Figure S6A. hRAR γ -selective chemical 4647 is selective on xRAR γ . (Top) Cos7 cells were transfected with 5:5:1 DNA ratio of reporter : β -gal : xRAR^{EGCKG→GSCKV} (or *mCherry* control), and treated with 10 μ M-10 fM 4647 or vehicle (0.1% DMSO). The y-axis is the relative light units measured by the luminometer divided by β -gal activity. The region of xRAR γ -selectivity is the concentration of 4647 that activates xRAR γ 1 and xRAR γ 2 but fails to activate xRAR α 1 and RAR α 2. (Bottom) Schematic of the full-length mutant RAR^{EGCKG→GSCKV} system using the (RXRE^{1/2}-GRE^{1/2})x4 TK-Luciferase reporter.

Supplemental Figure S6B



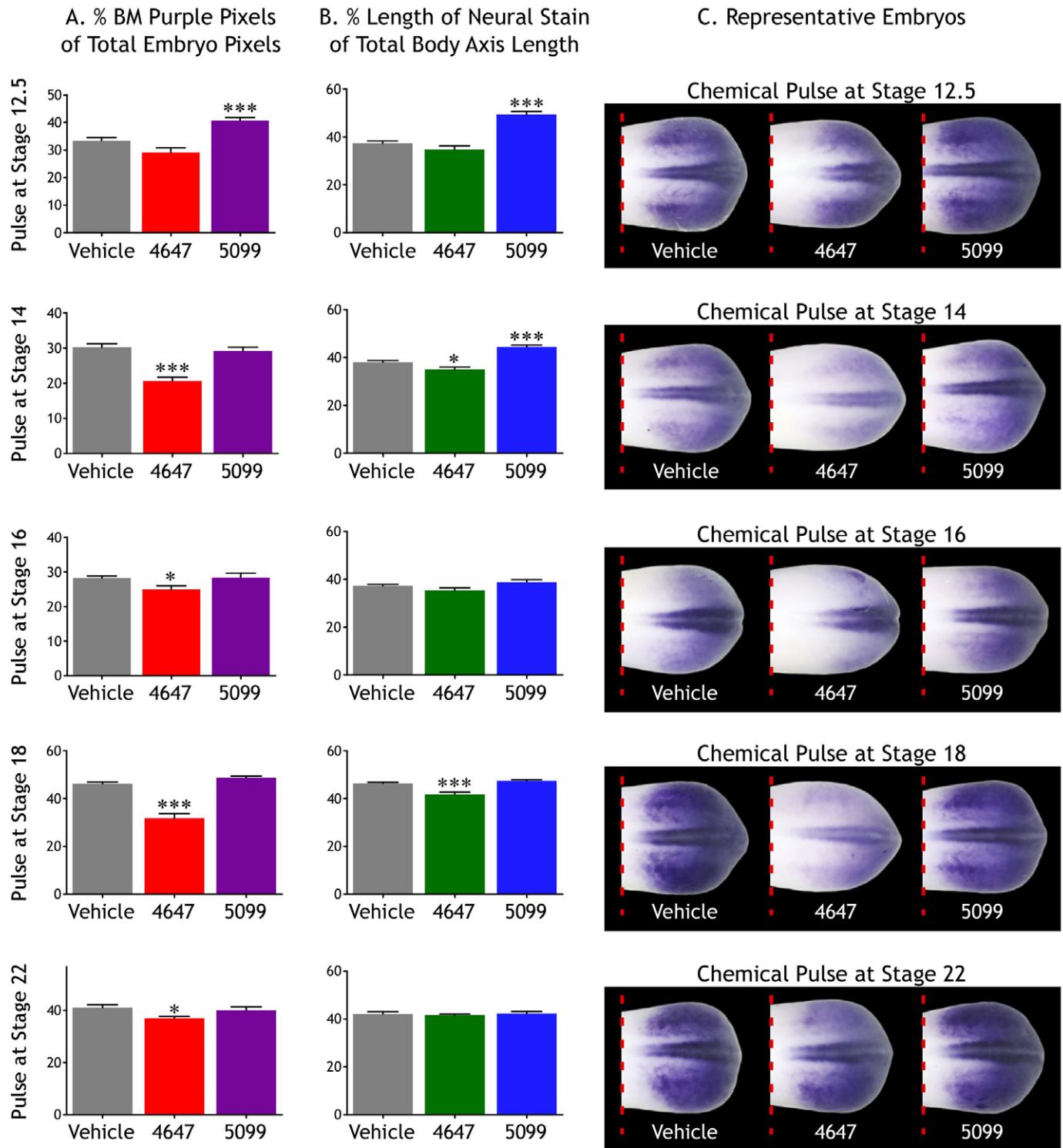
Supplemental Figure S6B. hRAR γ -selective chemical 5099 is selective on xRAR γ . (Top) Cos7 cells were transfected with 5:5:1 DNA ratio of reporter : β -gal : xRAR^{EGCKG→GSCKV} (or *mCherry* control), and treated with 10 μ M-0.1 nM 5099 or vehicle (0.1% DMSO) against 10 nM 9-cis RA. The y-axis is % reduction (100% = 9-cis RA alone) of relative light units divided by β -gal activity. The region of xRAR γ -selectivity is the concentration of 5099 that represses xRAR γ 1 and xRAR γ 2 but fails to repress xRAR α 1 and RAR α 2. (Bottom) Schematic of the full-length mutant RAR^{EGCKG→GSCKV} system using the (RXRE^{1/2}-GRE^{1/2})x4 TK-Luciferase reporter.

Supplemental Figure S7



Supplemental Figure S7. Expression of *Hoxc13* across developmental time. WISH of *Hoxc13* mRNA expression at developmental stages 16 (A, B), 22 (C, D), and 30 (E, F). Dorsal (A, C, F) and lateral (E) views are shown with anterior to the left. Caudal (B, D) views are shown with dorsal at the top. (G) QPCR showing developmental expression of *Hoxc13*. The y-axis represents $2^{-\Delta Ct}$ values, normalized to reference gene, *Histone H4*.

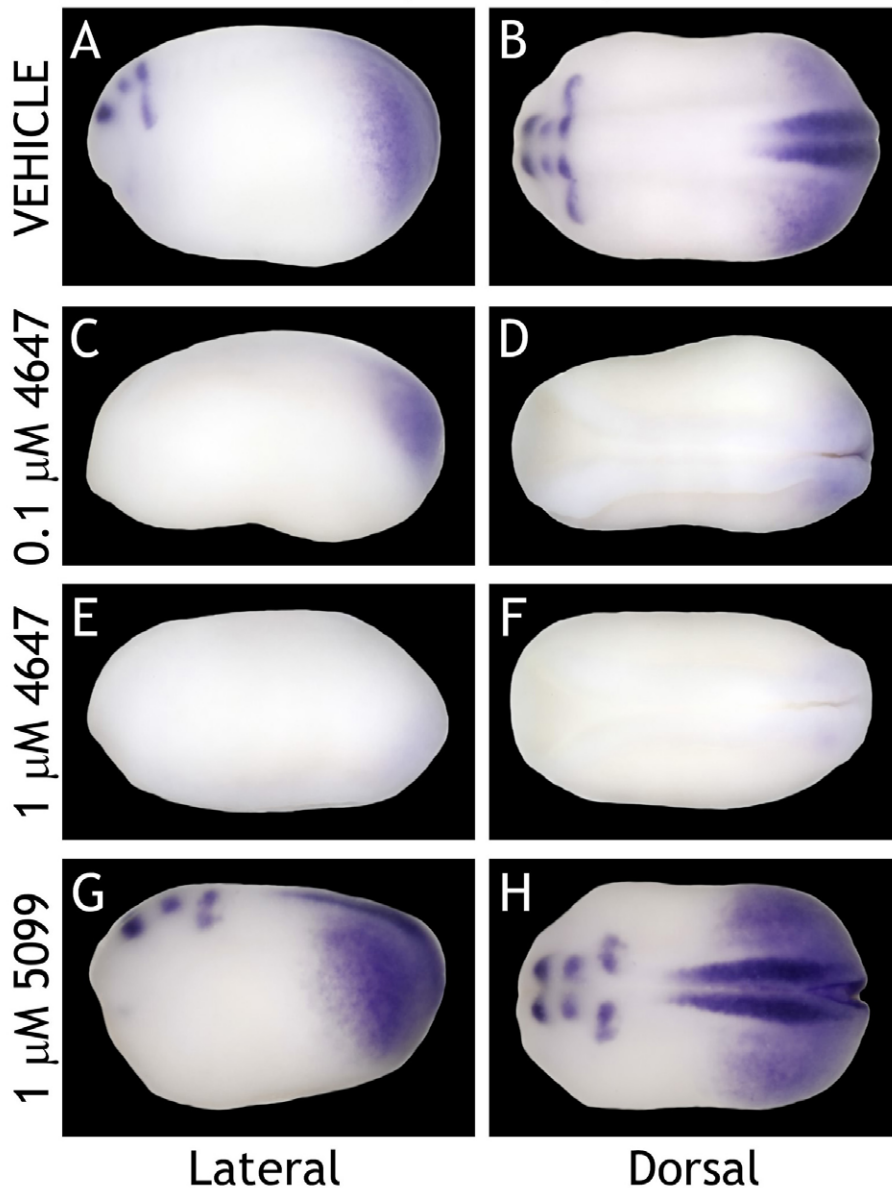
Supplemental Figure S8



Supplemental Figure S8. Pulse treatments determine short-term effects of 4647 and 5099. WISH from embryos treated for one hour at stage 12.5, 14, 16, 18, and 22 with 10 nM 4647, 0.5 μ M 5099, or vehicle (0.1% EtOH). **(A)** Quantitation of purple pixels with respect to total embryo body pixels. **(B)** Quantitation of *Hoxc10* neural stain length with respect to total body axis length. Statistical significance was determined using 1-way ANOVA in GraphPad Prism v5.0. (* = $P \leq 0.05$, *** = $P \leq 0.001$). **(C)** Representative embryos from this experiment. Embryos shown in dorsal view at tailbud-stage; anterior on left. Dashed red line represents 1/2 the embryo axis.

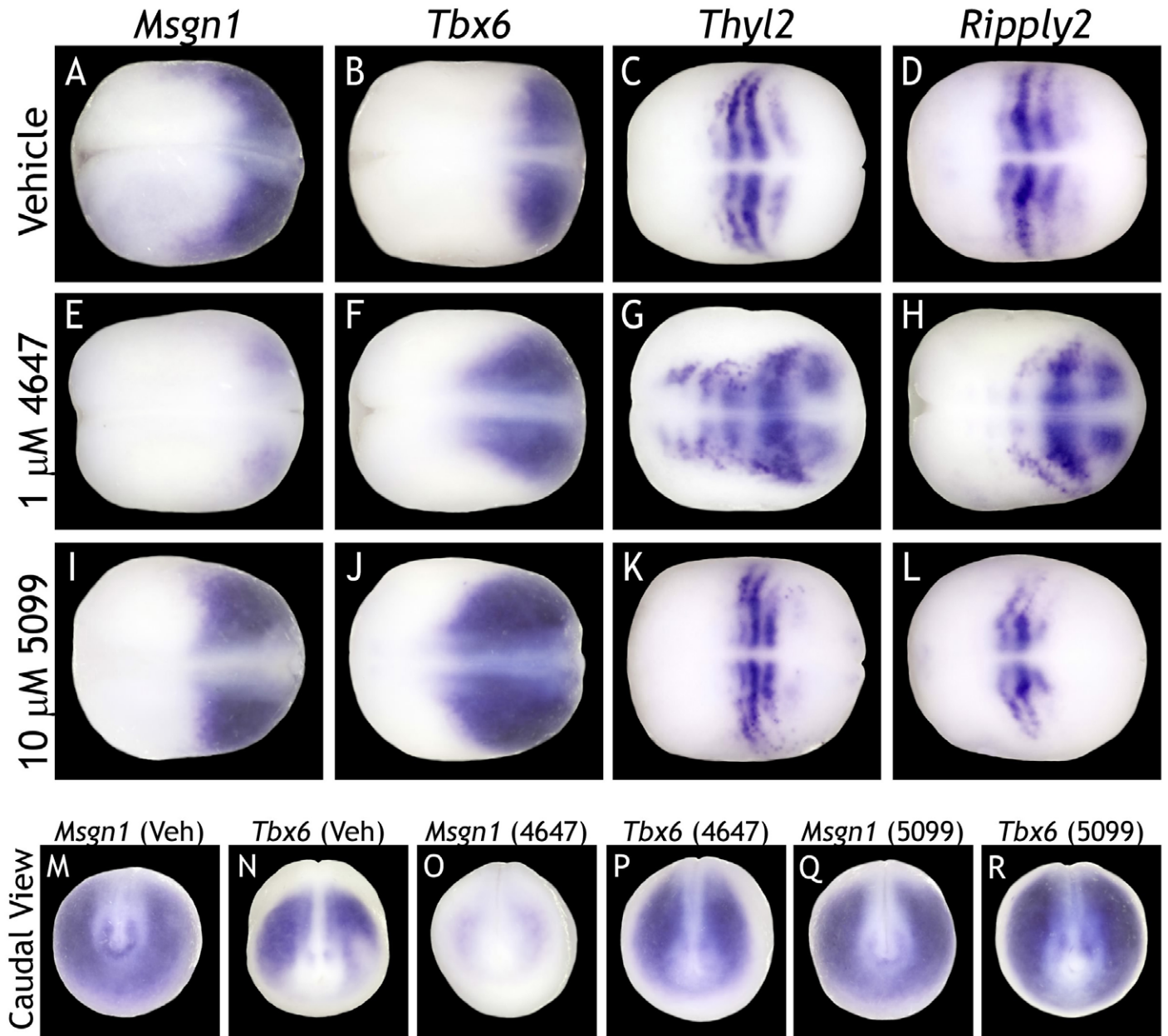
Supplemental Figure S9

Hoxc10, *Krox20*, *En2*



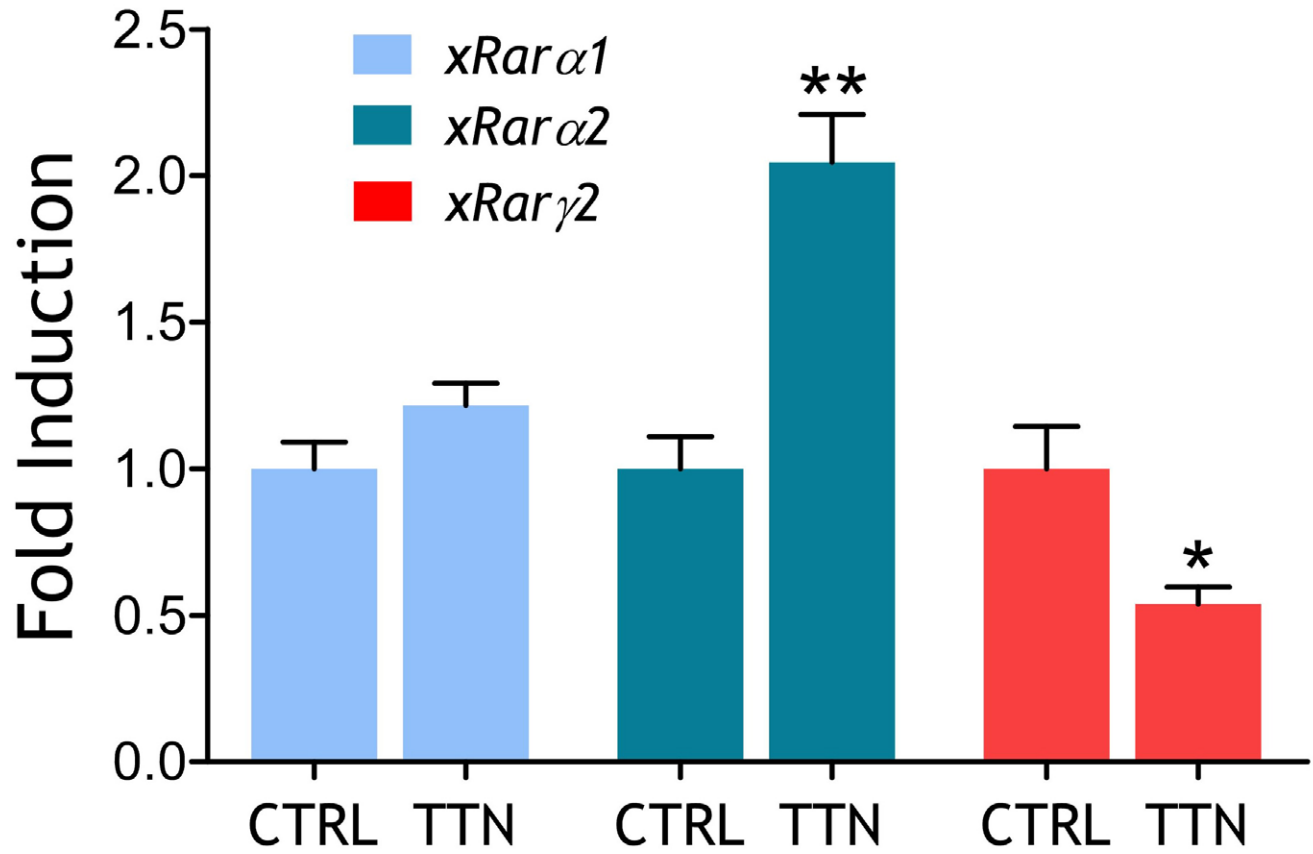
Supplemental Figure S9. *Hoxc10*, *Krox20*, and *En2* expression domains are reduced by 4647 and expanded by non-receptor-selective doses of 5099. (A-H) WISH from embryos treated post-gastrulation (stage 12.5) with non-receptor-selective doses of 4647, 5099, or vehicle (0.1% EtOH). (A, B) Control expression of *Hoxc10*, hindbrain marker *Krox20*, and midbrain marker *En2*. (C-F) 0.1 μM 4647 diminishes (14/14), and 1 μM knocks out (15/15), expression of *Hoxc10*. 0.1 μM and 1 μM doses obliterate *Krox20* and *En2* (0.1: 14/14; 1: 15/15). (G, H) 1 μM 5099 rostrally expands expression of *Hoxc10* and caudally expands *Krox20*, and *En2* (14/15). Embryos are shown in lateral or dorsal view at tailbud-stage; anterior is on the left.

Supplemental Figure S10



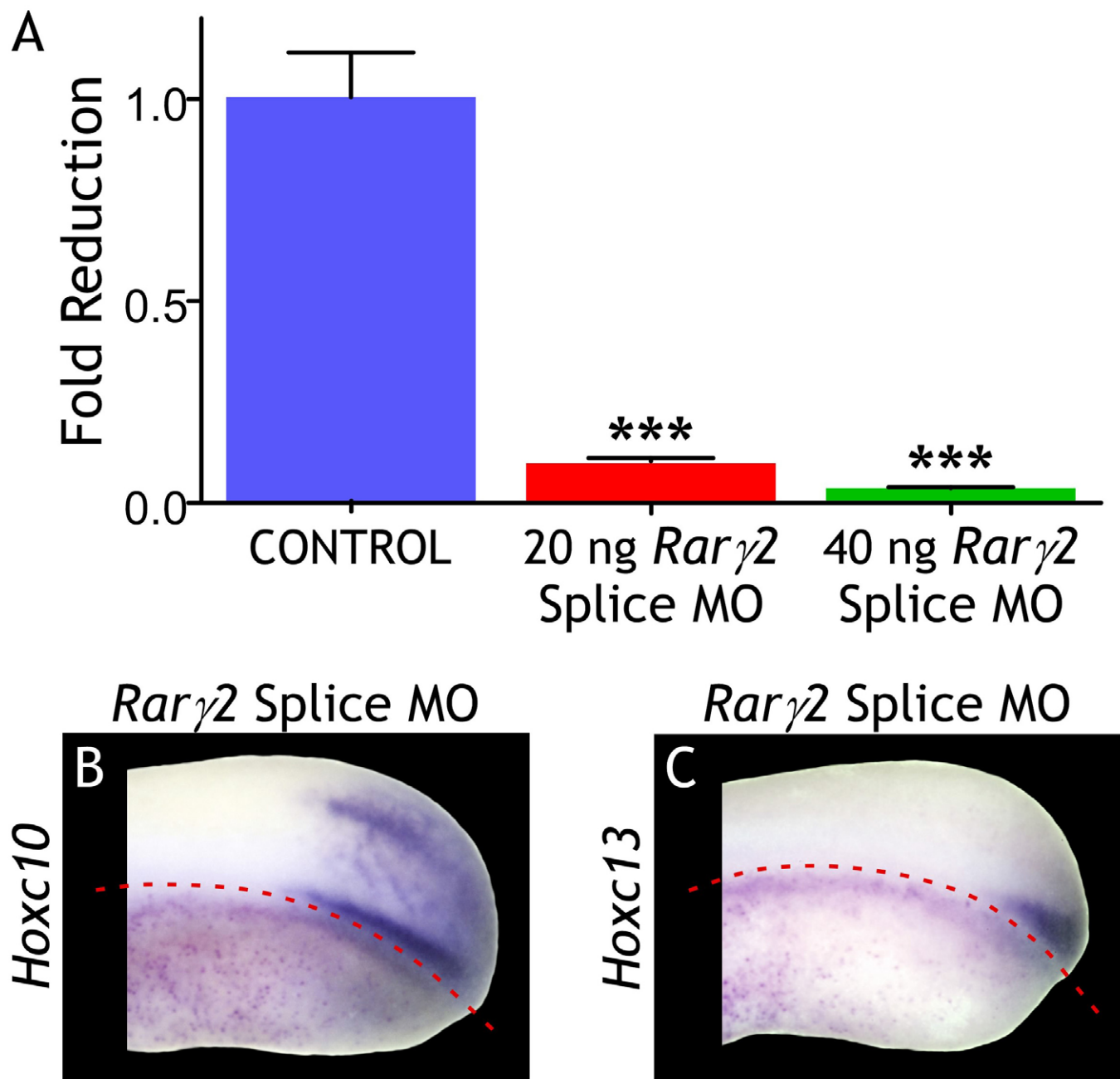
Supplemental Figure S10. Presomitic mesoderm markers are significantly altered by 4647 and 5099. (A-R) WISH from embryos treated post-gastrulation (stage 12.5) with non-receptor-selective doses of 4647, 5099, or vehicle (0.1% EtOH). (A-D) Control expression of *Msgn1*, *Tbx6*, *Thyl2* and *Ripply2*. (E) *Msgn1* expression is diminished by 4647 (15/15 embryos). (F) *Tbx6* expression is expanded by 4647 (17/17). (G, H) Somitomere domains of *Thyl2* (20/20) and *Ripply2* (21/21) are thicker, posteriorly expanded, and lack lateral expression. Anterior, ectopic somitomeres are visible in 60% of embryos. (I, J) *Msgn1* (15/15) and *Tbx6* (17/17) expression are expanded with 5099. (K, L) Somitomere domains of *Thyl2* (18/18) and *Ripply2* (17/17) are reduced in number and thinner. Embryos are shown in dorsal view at neurula-stage; anterior is on the left. (M-R) Caudal views of *Msgn1*, and *Tbx6*.

Supplemental Figure S11



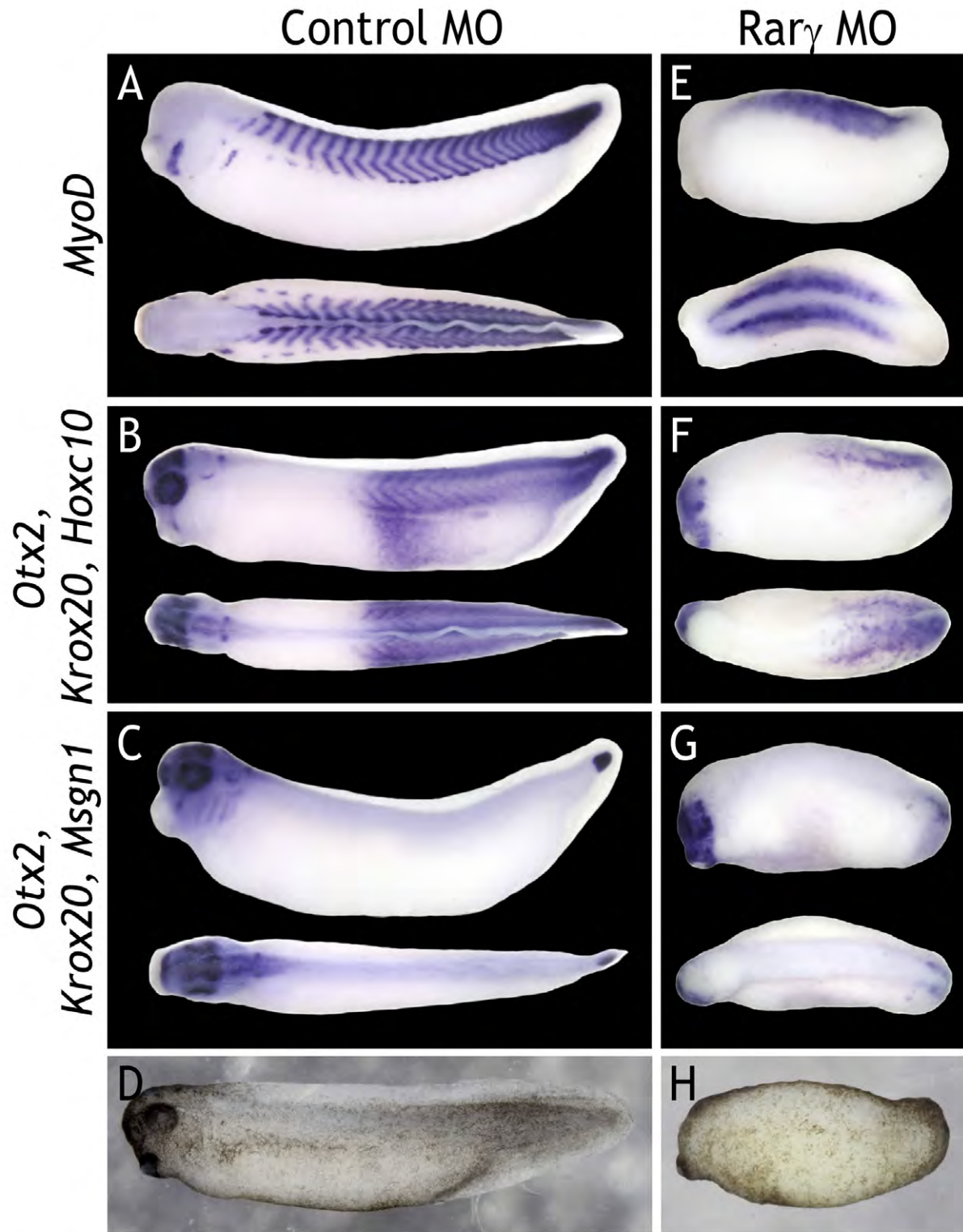
Supplemental Figure S11. *Rary2* is not inducible by TTNPB. PCR showing *xRara1*, *xRara2*, and *xRary2* expression in embryos treated at stage 7/8 with 1 μ M TTNPB or vehicle (0.1% EtOH). The y-axis represents $2^{-\Delta\Delta Ct}$ values normalized to *Histone H4* and expressed as fold induction relative to control. *xRara2* is induced by TTNPB whereas *xRary2* is repressed by TTNPB. Statistical significance was determined using unpaired t-test in GraphPad Prism v5.0 (* = $P \leq 0.05$, ** = $P \leq 0.01$).

Supplemental Figure S12



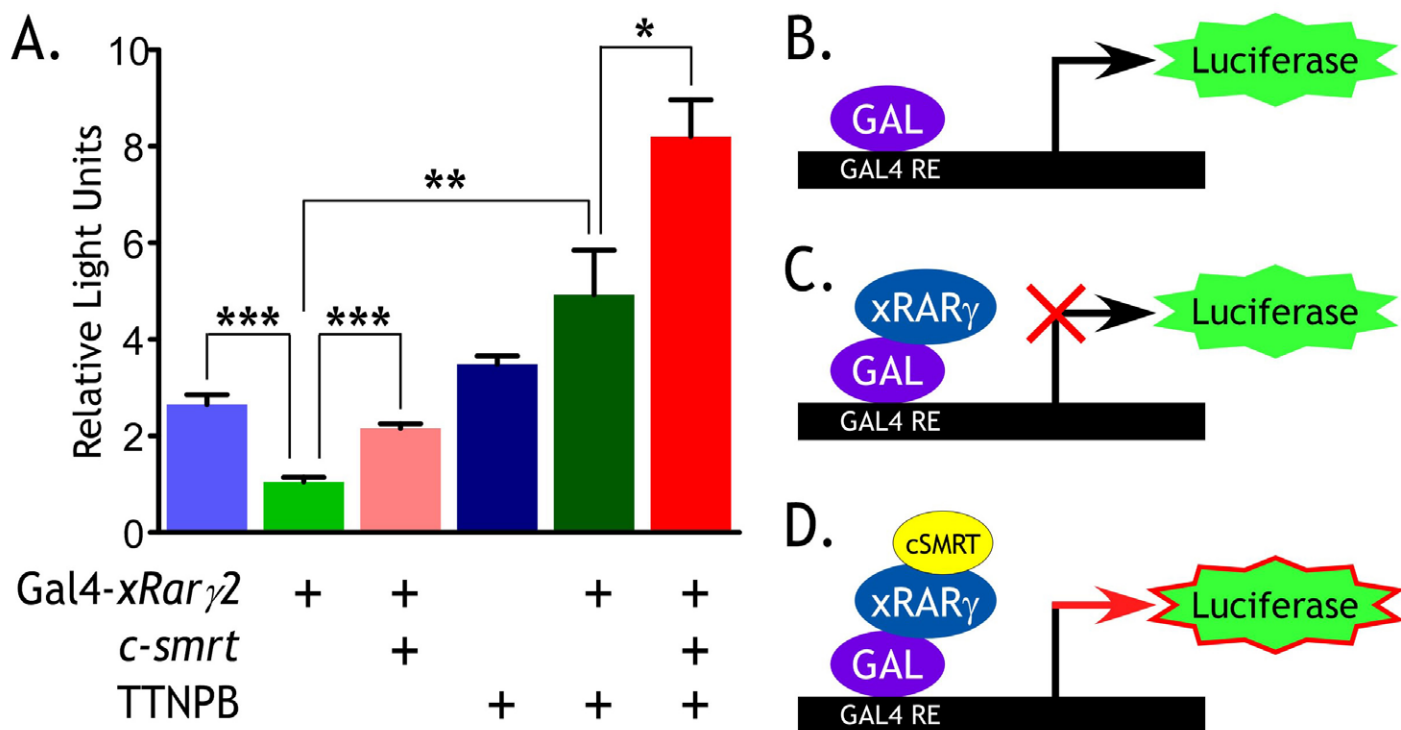
Supplemental Figure S12. *Rary2* splice MO significantly reduces *Rary2* expression. (A) QPCR of cDNA of uninjected embryos or embryos bilaterally injected with *Rary2* splice MO. The y-axis represents $2^{-\Delta\Delta Ct}$ values normalized to *Histone H4* and expressed as fold reduction relative to control. 20 ng and 40 ng of *Rary2* splice MO yielded significant reduction of *Rary2* expression. Statistical significance was determined using unpaired t-test in GraphPad Prism v5.0 (***) = $P \leq 0.001$). Primer sequences are found in **Table S6**. (B, C) Embryos were injected unilaterally at the 2- or 4-cell stage with 40 ng *Rary2* splice MO. The injected side is indicated by the magenta β -gal lineage tracer. *Rary2* splice MO resulted in curved axes on the injected side, and decreased expression of *Hoxc10* (14/14 neural KD, 8/14 lateral KD, 6/14 lateral blurring) and *Hoxd10* (26/26 KD/KO).

Supplemental Figure S13



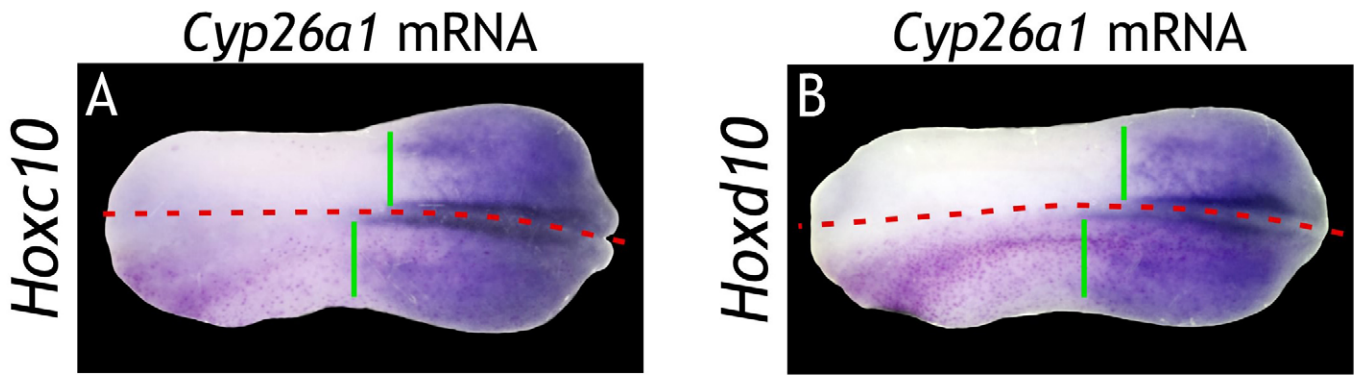
Supplemental Figure S13. Embryos were injected bilaterally at the 2-cell stage with 5 ng *Rary* MO or Control MO. Control MO did not alter expression of (A) *MyoD*, (B) *Otx2*, *Krox20*, and *Hoxc10*, and (C) *Otx2*, *Krox20*, and *Msgn1* in stage-33 embryos. *Rary2.1/2.2* MO resulted in blurred and reduced somite domains (E), and diminished head and tail patterning (F, G) in stage-33 embryos. Embryos are shown in dorsal and lateral views with anterior on the left. (D, H) Unbleached, unstained embryos.

Supplemental Figure S14



Supplemental Figure S14. c-SMRT relieves repression of xRAR γ 2. (A) Embryos were injected unilaterally at the 2- or 4-cell stage with 50 pg reporter DNA, and 50 pg Gal4-*xRar* γ 2 mRNA +/- 4 ng *c-smrt* mRNA then treated at stage 9 with 1 μ M TTNPB or vehicle (0.1% EtOH). Basal reporter activity (A, B) is repressed by xRAR γ 2 (A, C). (A, D) c-SMRT relieves repression of xRAR γ 2, and this effect is potentiated by TTNPB. Statistical significance was determined using unpaired t-test in GraphPad Prism v5.0 (* = $P \leq 0.05$, ** = $P \leq 0.01$, *** = $P \leq 0.001$).

Supplemental Figure S15



Supplemental Figure S15. *Cyp26a1* mRNA overexpression expands posterior Hox gene expression domains. Embryos were injected unilaterally at the 2- or 4-cell stage with 1 ng *Cyp26a1* mRNA. The injected side is indicated by the magenta β -gal lineage tracer. **(A, B)** *Cyp26a1* mRNA overexpression resulted in rostral shifting (green lines) of the neural/midline and/or lateral domains of *Hoxc10* (12/12 embryos) and *Hoxd10* (10/11) expression. Embryos are shown in at tailbud-stage with anterior on the left.

Supplemental Table 1. Morpholinos

MO	Type	Sequence (5'→3')
<i>Rary1</i>	AUG	GCT GTT TGC CAT TGC CTT GTT CTA
<i>Rary2</i>	AUG	TTC CAT GCA GTC ATA CAT TTT GGG
<i>Rary</i>	Splice	GGG TAA CAC TTA CCT TGC AAC CTT C

Supplemental Table 2. xRAR β cloning primers

Primer	pCMX-GAL4-xRAR β Sequence (5'→3')
Forward	TCG CCG GAA TTC TCC AAA GAA TCC GTC AGA AAT G
Reverse	TGG CCA GGA TCC TAT TGA ACC TGT GCA CAT TTA CTA AC
Primer	pCDG1-xRAR β Sequence (5'→3')
Forward	CAG ATA CCA TGG GAA TGT TTG ACT GTA TGG ATG TTC TG
Reverse	ACT AGT GGA TCC TAT TGA ACC TGT GCA CAT TTA CTA AC

PCR Template = *Xl*. cDNA

Supplemental Table 3. Two-Frag PCR of pCDG1-xRAR^{EGCKG→GSCKV}

Primer	xRARα1 ^{EGCKG→GSCKV} or xRARα2 ^{EGCKG→GSCKV} (5'→3')
A (α 1)	CAG ATA CCA TGG CCA GTA AGG ACA A
A (α 2)	CAG ATA CCA TGG TCA GTT TGG ATT TCA G
B	CAC CTT GCA ACT TCC ACA AGC GCT GAC TCC ATA GT
C	GCT TGT GGA AGT TGC AAG GTG TTT TTC CGT CGC AGT ATC CAG
D	ACT AGT GGA TCC TCA GGG TGA GT

PCR Template = pCDG1-xRAR α 1 or pCDG1-xRAR α 2

Primer	xRARβ2 ^{EGCKG→GSCKV} (5'→3')
A	CAG ATA CCA TGG GAA TGT TTG ACT GTA TGG ATG TTC TG
B	CAC CTT GCA ACT TCC ACA TGC ACT GAC TCC ATA GTG ATA
C	GCA TGT GGA AGT TGC AAG GTG TTC TTC CGG CGG AGT ATT CAG AA
D	ACT AGT GGA TCC TAT TGA ACC TGT GCA CAT TTA CTA AC

PCR Template = XI. cDNA

Primer	xRARγ1 ^{EGCKG→GSCKV} or xRARγ2 ^{EGCKG→GSCKV} (5'→3')
A (γ 1)	CAG ATA CCA TGG CAA ACA GCA GCA AG
A (γ 2)	CAG ATA CCA TGG GAA TGT ACG ACT G
B	CAC CTT GCA ACT TCC GCA TGA ACT GAC CCC GTA GT
C	TCA TGC GGA AGT TGC AAG GTG TTT TTT CGG CGC AGT ATA CAG AA
D (γ 1)	ACT AGT GGA TCC GAT ATC TTT CCC CAA TAT G
D (γ 2)	ACT AGT GGA TCC CTA AGG GTT CTT C

PCR Template = pCDG1-xRAR γ 1 or pCDG1-xRAR γ 2

Supplemental Table 4. Probes with T7 adapters

Primer	Sequence (5'→3')
F (<i>xRARγ1</i>)*:	TTA CAG GAT CAC GTG AGA TTG AGC
R (<i>xRARγ1</i>)*:	taa tac gac tca cta tag ggT GCT GCA CCC ATG GTT AAA GAC
F (<i>xRARγ2</i>)*:	CTG TCT GCT ATC AGA GCC CAC
R (<i>xRARγ2</i>)*:	taa tac gac tca cta tag ggT GTG GCT CTG CAT CCA TCC
F (<i>Hoxc10</i>):	CCA ACA ATG TGA CTC CTA ACT CGT
R (<i>Hoxc10</i>):	taa tac gac tca cta tag ggT CAG TTC CCG AAT TCG GTT CTC
F (<i>Hoxd10</i>):	TTT CTA TTC TAA CAG CGC CAG CA
R (<i>Hoxd10</i>):	taa tac gac tca cta tag ggC ACT CTT ACT GAT CTC TAG GCG G
F (<i>Hoxa11</i>):	TAA TCC CTC CAA TGT CTA CCA CCC
R (<i>Hoxa11</i>):	taa tac gac tca cta tag ggG TGG TGG CAG ATA TCC GTC TC
F (<i>Hoxc13</i>):	AAC TGT GCA AGC AGC CAC TG
R (<i>Hoxc13</i>):	taa tac gac tca cta tag gCT GCG GTA GTT GCT CAC CTC
F (<i>Ripply2</i>):	GCA AGT GGT TTG CCA AGT CC
R (<i>Ripply2</i>):	taa tac gac tca cta tag ggT CAA ATC CAG AGT CTT GTT CCT CC
F (<i>Thylacine2</i>):	ACA CTT AAA CCA GAG TCT TTC ACC T
R (<i>Thylacine2</i>):	taa tac gac tca cta tag ggA TCT GAA GCT TTG CCT TCA GTG G
F (<i>Mesogenin</i>):	AAT GGA AGA GGA CTA TGC CTT GAG
R (<i>Mesogenin</i>):	taa tac gac tca cta tag ggT CTT GGA GCA CTG GAG AAG GT
F (<i>Tbx6</i>):	GGC ACC TCC TAC ACG ATG AGA C
R (<i>Tbx6</i>):	taa tac gac tca cta tag ggC TCC TCT TCC TGT TCC TGT TCC A
F (<i>MyoD</i>):	CAC TGC GGG ACA TGG AAG TC
R (<i>MyoD</i>):	taa tac gac tca cta tag ggG TAT TGC TGG GAG AAG GGA TGG T
F (<i>Raldh2</i>):	ACC CTT GAA TCT CTA AAC AGT GGC
R (<i>Raldh2</i>):	taa tac gac tca cta tag ggA ATC TCT TCT CTG GCA ATC CGC A

*Sense probes were PCR amplified from same primers except the T7-adaptor was moved to the forward, 5' end.

Supplemental Table 5. QPCR and PCR primers

QPCR

Primer	Sequence (5'→3')
F (<i>xRARα1</i>):	CCA CAT ATG TTG GGG GGT ATG TC
R (<i>xRARα1</i>):	GAT TCT GGG GAG CGG TGG T
F (<i>xRARα2</i>):	CCA CTC AAT TGA GAC TCA GAG CAC
R (<i>xRARα2</i>):	CTC TTG TCC TGA CAC ACA AAG CA
F (<i>xRARβ1</i>):	TTT CCT CCT GTC ATT GGT GGA CTC
R (<i>xRARβ1</i>):	GCT CTG GGT TTC GAT GGT TGC
F (<i>xRARβ2</i>):	CAA ATG CTG GAT TTC TAC ACT GCG
R (<i>xRARβ2</i>):	GTG TTG CCA TTC TGT CTG TGC C
F (<i>xRARγ1</i>):	AGA ACA AGG CAA TGG CAA ACA G
R (<i>xRARγ1</i>):	GCA AGT ACT TCA AAT GGT GGA GAT C
F (<i>xRARγ2</i>):	GTA GAA ACA CAA AGT ACC AGC TCG
R (<i>xRARγ2</i>):	CCG TAG TGA TAA CCT GAA GAC TTG T
F (<i>xHoxc13</i>):	AAG GCT ACC AAC ACT GGG CTC
R (<i>xHoxc13</i>):	GAC CAC ATC TGG GAA AGG TGC
F (<i>Histone H4</i>):	GAT AAC ATC CAG GGC ATC AC
R (<i>Histone H4</i>):	TAA CCT CCG AAT CCG TAC AG

PCR

Primer	Sequence (5'→3')
F (<i>xRARγ2_Splice</i>):	GCC GCT CTA TGA CAT GAG TCC
R (<i>xRARγ2_Splice</i>):	TTC CTC CGA GCT GGT ACT TTG TG